CRITICAL SPEEDS AND STABILITY OF ROTATING SHAFTS BY FEM

by

VIJAYAKUMAR MAHENDRAKER

DEPARTMENT OF MECHANICAL ENGINEERING

INDIAN INSTITUTE OF TECHNOLOGY, KANPUR

NOVEMBER, 1988

CRITICAL SPEEDS AND STABILITY OF ROTATING SHAFTS BY FEM

by

VIJAYAKUMAR MAHENDRAKER

DEPARTMENT OF MECHANICAL ENGINEERING

INDIAN INSTITUTE OF TECHNOLOGY, KANPUR

NOVEMBER, 1988

CRITICAL SPEEDS AND STABILITY OF ROTATING SHAFTS BY FEM

A Thesis Submitted
In Partial Fulfilment of the Requirements
for the Degree of

MASTER OF TECHNOLOGY

by

VIJAYAKUMAR MAHENDRAKER

to the

DEPARTMENT OF MECHANICAL ENGINEERING
INDIAN INSTITUTE OF TECHNOLOGY, KANPUR
NOVEMBER, 1988

ME - 1988- M- MAH - CRJ

15/11/88

CERTIFICATE

This is to certify that the present work "Critical Speeds and Stability of Rotating Shafts by FEM" has been carried out by Mr. Vijayakumar Mahendraker under my supervision and it has not been submitted elsewhere for a degree.

Bhupinder Pal Singh. Nov. 15, 8

(BHUPINDER PAL SINGH)
Professor
Department of Mechanical Engineer
I.I.T. KANPUR-208016

November, 1988

ACKNOWLEDGEMENTS

I am deeply indebted to my guide Dr. B.F. Singh, Department of Mechanical Engineering, for his invaluable guidance, constant cooperation and inspiration throughout the course of this work. The memory of the cordial relation with him will be cherished by me forever.

I thank Mr. K.G. Shastry for useful discussions with him during the course of this work. I acknowledge the helps rendered by Mr. K.R. Upadhyaya while preparing this manuscript. I wish to express my thanks to all those who have helped directly or indirectly.

I take this opportunity to thank all my friends for making my stay a pleasure at I.I.T. Kanpur. I cherish the homely atmosphere created by the members of the family of faculty from Karnataka and Mr. B.P. Nandwana and family.

I also take this opportunity to thank Mr. H.V.C. Srivastava for his neat and patient typing.

Vijayakumar Mahendraker

CONTENTS

LIST OF TABLES

LIST OF FIGURES

NOMENCLATURE

A	Area of cross section
A_o	Area of cross section at S = 0
$[C]^{(e)}$	Elemental damping matrix
C_{xx}, C_{yy}	Non-dimensional bearing damping coefficients
EI	Flexural rigidity of shaft
G	Shear modulus
$[G]^{(e)}$	Elemental gyroscopic matrix
h	Length of finite element
I_D	Diametral mass moment of inertia per unit length
I_p	Polar mass moment of inertia per unit length
I_o	Area moment of inertia at S = 0
I_1	Area moment of inertia in plane IIS
I_2	Area moment of inertia in plane IS
K'	Transverse shear form factor
$[K]^{(e)}$	Elemental stiffness matrix
k	Radius of gyration of mass moment of inertia
k_1	Radius of gyration of area moment of inertia I_1
K_{xx}, K_{yy}	Non-dimensional bearing stiffness values

l	Length of shaft
m	Mass per unit length
Mc	Material constant
$[M]^{(e)}$	Elemental mass matrix
$[N]$	Shape functions
$\{q\}^{(ne)}$	Nodal displacement vector
Re	Rotatory inertia coefficient
s	Position along length
S	Position along length in non-dimensional form
T_e	Total kinetic energy
t	Time
T	Non-dimensional time
T^*	Non-dimensionalisation factor
U	Strain energy of shaft
x,y	Translation of mass centre of shaft along OX and OY axes
z	Translation in the complex form
Z	Non-dimensional form of z
β_x, β_y	Angles of destortion due to shear deformation in YS and XS planes
δ	Variational operator
ϕ	Bending slope in the complex form

Ω	Non-dimensional spin speed
Ω_o	Spin speed of shaft
θ_x, θ_y	Bending slopes in YS and XS planes
θ_ξ	Bending slope in IIS plane
θ_η	Bending slope in IS plane
ρ	Mass density
ρ_c	Radius of curvature
σ_s	Normal stress on shaft cross section
ε_s	Normal strain on shaft cross section
ξ_o	Translation along IS axis
ξ	Translation along IS axis in non-dimensional form
η_o	Translation along IIS axis
$\bar{\eta}$	Translation along IIS axis in non-dimensional form
η_V	Internal viscous damping coefficient
η_{VN}	Internal viscous damping coefficient in non-dimensional form
η_H	Loss factor
γ_H	Loss angle
λ	Natural frequency in XYS frame
λ'	Natural frequency in I IIS frame
$(\dot{.})$	Differentiation with respect to time
$(.')$	Differentiation with respect to position

SYNOPSIS

In this work critical speeds of rotating shafts are obtained. Isotropic and anisotropic (dissimilar stiffness in two principal directions) shafts are onsidered. Various factors affecting the critical speeds are taken into account and their effects are studied.

The relevant governing differential equations are derived and FEM has been used for their solution. Galerkin's technique is used to minimise the residues obtained by finite element approximation. The element matrices are integrated numerically using Gauss quadrature, assembled and solved for frequencies and critical speeds for various boundary condition

The factors affecting the critical speeds considered for the present study are shear deformation, rotatory inertia and gyroscopic moments. Shaft with dissimilar support conditions in two principal planes has also been studied. An attempt to estimate the errors due to the assumptions of massless shaft and rigid disk has been done. The critical speeds for multiple span shafts are also obtained.

The effect of internal damping on the stability has been studied. Both viscous form and hysteretic form of internal damping are considered. The effect of bearing charecteristics (stiffness and damping) on the instability threshol has been studied.

CHAPTER- I

INTRODUCTION

1.1 THE PROBLEM IN BRIEF :

It was recognised early in 18th century that, a rotating shaft initiated vibrations of large amplitudes at certain speeds and often caused catastrophic failure of supporting structure and other parts of the system. The operating speeds at which this phenomenon occured, came to be known as critical speed.

A shaft always has certain amount of mass unbalance, which during rotation, deflects the shaft axis from its equillibrium position. This leads to transverse vibration of shaft at its natural frequencies. In general the natural frequencies of a rotating shaft are dependent on speed of rotation. The vibrations of shaft along any two mutually perpendicular directions in the plane of cross section, occur at same frequency, but with a phase difference of $\pm \frac{\pi}{2}$ Due to this, the shaft axis begins to precess about the line joining the supports, with a speed equal to the anguler frequency of natural vibrations. The precession of shaft can be in the same direction as that of spin of shaft or in the opposite direction. When precession is in same direction

as that of spin, it is termed as forward precession and when in opposite direction, it is called as backward precession.

The inertia force due to unbalance has the frequency of spin speed of shaft. Hence, when the speed of precession of shaft becomes equal to the spin speed, resonant state is reached, i.e. amplitude grows linearly with time. When this state arises, the corresponding spin speed of shaft is called as critical speed, Depending upon the direction of precession, it is termed as forward critical speed or backward critical speed.

1.2 LITERATURE REVIEW :

The first published work related to this problem was in 1869, by Rankine [1], The operating speeds of rotating machinery were below the first critical speed in those days. Hence, most of the early work in this field is limited to the determination of first critical speed. However, with the advent of new technology in the field of rotating machinery, the present day operating speeds are far in excess of first critical speed. Consequently, the more recent literature treats a greater range of problems related to rotating shafts, such as effect of various system parameters on critical speeds, determination of stable operating speed ranges, causes of instabilities and methods to improve the stabilities. Thus the study of vibratory motion becomes necessary, for stable and safe operation of rotating machinery.

A very good survey of work done in this field till 1967, can be found in the monograph "Dynamics of rotating shaft" by Loewy and Piarulli [2]. This monograph tries to illustrate the basics of rotor dynamics. It neglects the mass of the shaft, i.e., it uses lumped mass approach. It provide general but qualitative information on the effects of various parameters on critical speeds and stability. It also treats coupled, lateral and torsional motion and balancing.

A more involved and analytical study of the problems of rotor dynamics is found in the work of Tondl [3] . The book gives a good insight of several phenomena of rotor dynamics. The topics emphasised in his work are, effect of internal damping, effect of unequal shaft stiffness and effect of oil film in journal bearings. It deals comprehensively with problems concerned with the stability of rotor motion, with the creation of self excited vibration, and with non-linear resonances. But almost the whole book is based on the assumption of massless shaft and rigid disk. All the same, the book gives an excellent review of the problems, supplemented with results of experimental investigations. Combined effect of torsional and flexural rigidities, combined effect of several factors, causing instability have been dealt in detail.

Another very prominent contribution in this field is of Dimentberg [4] . This work deals with flexural transverse vibration. Major part of the book uses continuous approach. Closed form solutions, for hinged-hinged support conditions, for several cases are obtained. This book showed, the limitation of critical speeds in forward precession of a shaft with uniformly distributed mass, was a result of neglecting the effect of shear deformation. Effect of external and internal damping, effect of dissimilarity of stiffness, effect of dissimilar fixing conditions in two planes multi-bearing systems, are few of the cases studied in his work. Further, both uniform stiffness and dissimilar stiffness shafts are analysed with and without consideration to shear deformation effect.

Another recent text in this field is of Rao [5] It uses lumped mass approach.

An excellent collection of papers on several problems of rotor dynamics, presented at an international symposium held at Denmark in 1974, can be found in the book edited by Niordson [6].

The application of FEM to the problems related to rotor dynamics was done by Ruhl and Booker [7] , in 1972. They analysed stability and unbalance response of a turborotor system. But the model used, included only translational kinetic energy and elastic bending energy i.e. used Euler beam theory. Nelson [8] improved the model by incorporating

the effect of rotatory inertia and gyroscopic action. Formulation is done using energy method. The effects of bearing stiffness and damping are also incorporated. Zorzi and Nelson [9], incorporated the effect of internal damping in the finite element model of [8]. According to [4] the possibility of instabilities in the post-critical speed range due to internal damping, was first shown by Kimball and Niwkirk [10]. The mechanism of internal damping is better represented by considering the hysteretic form, rather t viscous form [4]. A combined model incorporating both the forms of damping is formulated by [9]. A study of effect of bearing stiffness and damping charecteristics on the instability threshold is done by them. Later in 1985, Greenhill, Bickford and Nelson [11], extended the work of [9], for a shaft with variable cross section, by using a conical beam finite element.

There are a good number of authors who use transfer matrix method in this field. Lund [12], has studied the effect of fluid-film journal bearings and hysteretic internal damping, on the critical speeds and instability threshold. He also incorporated the effect of bearing stiffness and bearing damping. But he treats the shaft as a uniform beam, neglecting the effect of shear deformation, rotatory inertia and gyroscopic moments. Bansal and Kirk [13], improved this

work by incorporating the disk gyroscopic moments and shear deformation effect. Ramakrishnan and Prabhu [14] have studied the unbalance response, instability and critical speeds of multispan rotor systems.

All these authors, including Rao [5] use lumped mass approach in the transfer matrix method. Lumped mass approach is always less accurate than the distributed mass approach. Moreover this method requires some skill and experience as there are chances of missing some modes. Satisfaction of boundary conditions of intermediate supports is not very straight forward.

With continuous approach in transfer matrix method for beam problems, one faces some numerical problems. Moreover it is quite difficult (if not impossible) to obtain transfer matrices for rotors with rotatory, shear and gyroscopic effects. This difficulty is easily overcome in transfer FEM (TFEM) at the cost of little accuracy, Gupta [15] and Goel [16] . It eliminates the need of the solution over an element as it uses the finite element shape functions. Further, TFEM also has the advantage of lesser computer memory requirement as, the order of matrices to be handled remain same as in transfer matrix method. Thus the TFEM blends the advantages of FEM and transfer matrix method. But obtaining the complex frequencies for damped cases does not seem possible.

Recently, Goel [16]obtained the critical speeds of uniform, isotropic undamped shafts using Transfer FEM. The effects of shear deformation, rotatory inertia and gyroscopic moments were included in his analysis. It also covers multi-span shafts. In his work, two second order governing differential equations ,solved using linear polynomial , satisfying the continuity and completeness requirement led to ill-conditioning. To avoid this, these two equations were combined into a fourth order differential equation and cubic polynomial used. Although it was not possible to satisfy all the geometric and natural boundary conditions exactly in this approach, the results were quite satisfactory.

1.3 AIM AND SCOPE OF PRESENT WORK :

The present work aims at obtaining the critical speeds of flexible rotating shafts and studying the effect of various parameters on critical speeds. The relevant governing equations were derived and Galerkin FEM has been used to solve these more familier differential equations.

The effects of gyroscopic moments, rotatory inertia and shear deformation are incorporated. A study of critical speeds, neglecting the shear deformation is also done. Two second order governing equation approach is used in the preser work, except for the cases studied neglecting the effect of shear deformation.

For the vibration analysis of shafts, carrying disks having mass larger than shaft mass, the mass of shaft is generally neglected. An attempt has been made to estimate the error committed due to this assumption. For this, critical speeds for a range of ratios of shaft mass to disk mass are obtained. Further, the effect of flexibility of disk is also studied.

The effect of dissimilar shaft stiffness, caused by the unequal area moments of inertia of shaft section in the two principal planes is studied. The effect of dissimilarity in support conditions in the two planes is also included.

A study of instabilities caused by internal damping and the effect of bearing stiffness and damping properties on the stability are studied. Hysteretic, as well as viscous forms of damping are considered. The combined model incorporating both the forms, is formulated based on the work of Nelson [9]. The model is studied independently for both the forms of damping. Variation in instability threshold, with bearing stiffness and bearing damping is also studied.

CHAPTER- II

THEORY AND FORMULATION

This chapter gives the derivation of governing differential equations and corresponding FEM formulation of the various cases of shafts studied in this work.

2.1 ISOTROPIC SHAFT WITH NO DAMPING :

Governing differential equations for transverse vibrations of rotating shaft, incorporating the effects of shear deformation, gyroscopic moments and rotatory inertia are derived from Hamilton's principle.

Consider a differential element of length ds, as shown in Fig. (2.1). The kinetic energy of the shaft becomes [8].

$$T_e = \int_0^l \frac{1}{2} m\,(\dot{x}^2+\dot{y}^2)ds + \int_0^l \frac{1}{2} I_D(\dot{\theta}_x^2+\dot{\theta}_y^2)\,ds + \int_0^l \frac{1}{2} I_p\,\Omega_o^2 ds - \int_0^l I_p\,\Omega_o\,\dot{\theta}_x\theta_y\,ds$$

Here, m is the mass per unit length ; x and y are the translations along OX and OY axes ; I_D is the diametral mass moment of inertia per unit length ; θ_x and θ_y are the bending slopes in YS and XS planes; I_p is the polar mass moment of inertia per unit length and Ω_o is the spin speed, assumed constant. Dot represents the derivative with respect to time t. In the above Eqn. (2.1), the first term is the energy due to translation, second term is the energy due to rotatory inertia,

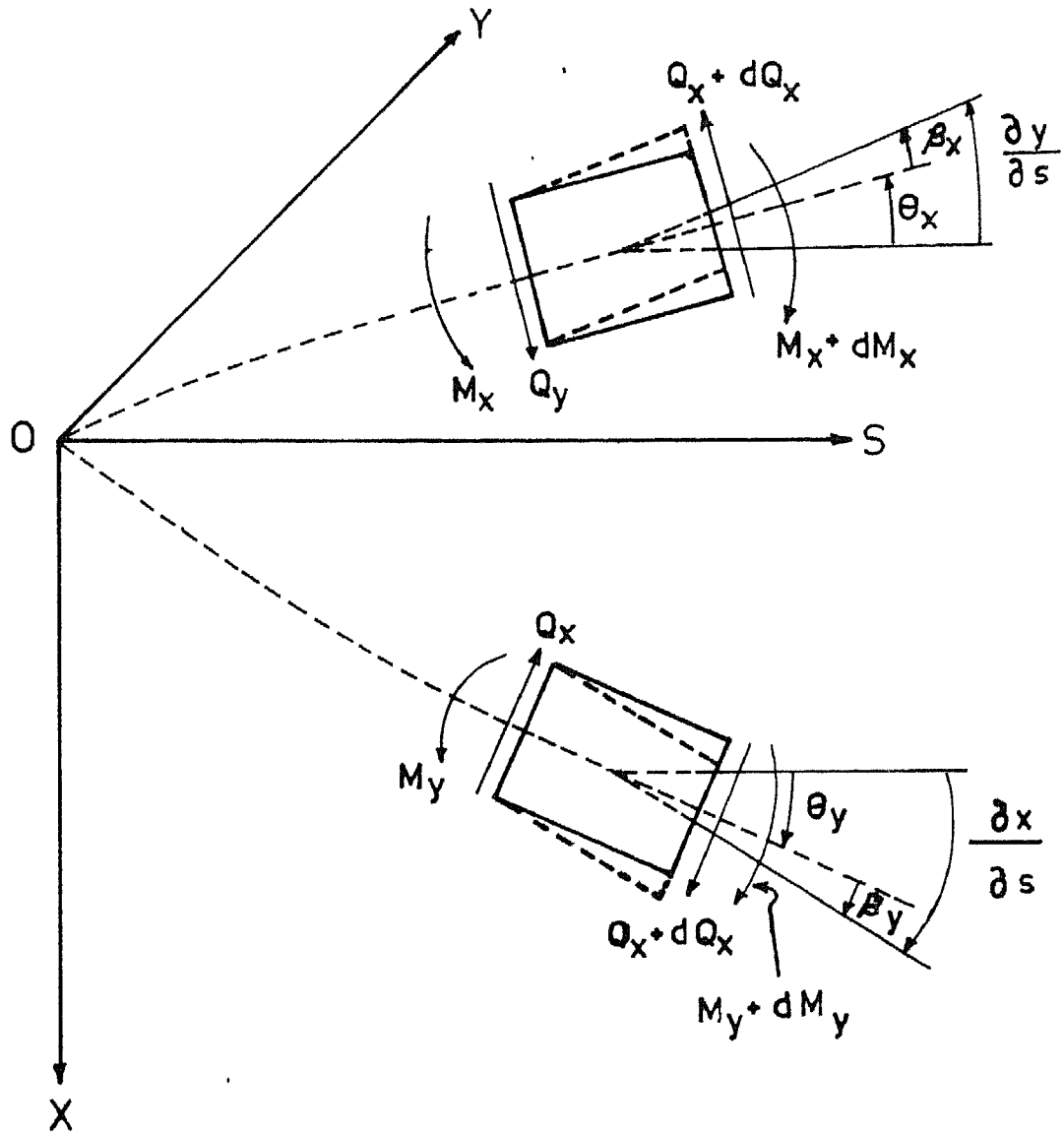

Fig. 2.1 Free body diagram of differential element in two planes

the third term is the energy due to spinning of the shaft and the last term gives the energy due to gyroscopic moments. Derivation of kinetic energy is given in Appendix I.

The strain energy of the shaft is

$$U = \frac{1}{2}\int_0^1 EI\,(\theta_x'^2 + \theta_y'^2)ds + \frac{1}{2}\int_0^1 K'GA\,(\beta_x^2 + \beta_y^2)\,ds \qquad \ldots. (2.2)$$

where EI is the flexural rigidity ; K' is transverse shear form factor, a constant depending upon the shape of cross section ; G is the shear modulus ; A is the area of cross section; β_x and β_y are the angles of distortion due to shear deformation about X and Y axes respectively. Strokes represent the derivatives with respect to S. First term in Eqn. (2.2) represents strain energy due to bending and the second term , strain energy due to shear deformation.

It is seen from the Fig.(2.1) that total slopes are

$$\begin{aligned} x' &= \theta_y + \beta_y \\ y' &= \theta_x + \beta_x \end{aligned} \qquad \ldots. (2.3)$$

Using Eqns. (2.3), expression for strain energy U given by Eqn. (2.2) becomes

$$U = \int_0^1 \frac{1}{2} EI(\theta_x'^2 + \theta_y'^2)ds + \int_0^1 \frac{1}{2} K'GA[\,(x' - \theta_y)^2 + (y' - \theta_x)^2\,]\,ds \qquad \ldots. (2.4)$$

Thus integral to be minimised is

$$I = \int_{t_1}^{t_2} (T_e - U)\,dt$$

$$\text{or } I = \int_{t_1}^{t_2} \int_{o}^{1} \left\{ \frac{1}{2} m(\dot{x}^2+\dot{y}^2) + \frac{1}{2} I_D(\dot{\theta}_x^2+\dot{\theta}_y^2) + \frac{1}{2} I_p \varrho_o^2 - I_p \varrho_o \dot{\theta}_x \theta_y - \frac{1}{2} EI (\theta_x'^2 + \theta_y'^2) - \frac{1}{2} K'GA \left[(x' - \theta_y)^2 + (y' - \theta_x)^2 \right] \right\} ds\, dt \quad \ldots\ldots (2.5)$$

By Hamilton's principle

$$\delta I = \delta \int_{t_1}^{t_2} (T_e - U) dt = 0 \quad \ldots\ldots (2.6)$$

Applying operator δ to Eqn. (2.5) is quite straight forward, but fourth term needs little special attention, and is

$$\delta \int_{t_1}^{t_2} \int_{o}^{1} I_p \varrho_o \dot{\theta}_x \theta_y \, ds\, dt$$

$$= \int_{o}^{1} \int_{t_1}^{t_2} I_p \varrho_o \delta(\dot{\theta}_x) \theta_y \, dt\, ds + \int_{t_1}^{t_2} \int_{o}^{1} I_p \varrho_o \dot{\theta}_x \delta\theta_y \, ds\, dt$$

$$= \int_{o}^{1} I_p \varrho_o \delta\theta_x \theta_y \Big|_{t_1}^{t_2} ds - \int_{o}^{1} \int_{t_1}^{t_2} I_p \varrho_o \delta\theta_x \dot{\theta}_y \, dt\, ds + \int_{t_1}^{t_2} \int_{o}^{1} I_p \varrho_o \dot{\theta}_x \delta\theta_y \, ds\, dt$$

$$= \int_{t_1}^{t_2} \int_{o}^{1} I_p \varrho_o (-\dot{\theta}_y \delta\theta_x + \dot{\theta}_x \delta\theta_y) \, ds\, dt \quad \ldots\ldots (2.7)$$

Thus, applying the δ operator to all terms in Eqn. (2.5) and rearranging, one gets

$$\int_{t_1}^{t_2}\int_{o}^{l}\{[-m\ddot{x}+(K'GA(x'-\theta_y))']\delta x$$

$$+[-I_D\ddot{\theta}_x+I_p\rho_o\dot{\theta}_y+(EI\theta_x')'+K'GA(y'-\theta_x)]\delta\theta_x$$

$$+[-m\ddot{y}+(K'GA(y'-\theta_x))']\delta y$$

$$+[-I_D\ddot{\theta}_y-I_p\rho_o\dot{\theta}_x+(EI\theta_y')'+K'GA(x'-\theta_y)]\delta\theta_y\}\ ds\ dt$$

$$-EI\,\theta_x'\,\delta\theta_x\Big|_o^l-EI\,\theta_y'\,\delta\theta_y\Big|_o^l$$

$$-K'GA(x'-\theta_y)\delta x\Big|_o^l-K'GA(y'-\theta_x)\delta y\Big|_o^l=0$$

.... (2.8)

The displacements δx, $\delta\theta_x$, δy and $\delta\theta_y$ are arbitrary, therefore

$$(K'GA(x'-\theta_y))-m\ddot{x}=0 \qquad \text{.... (2.9)}$$

$$(EI\,\theta_y')'+K'GA(x'-\theta_y)-I_D\ddot{\theta}_y-I_p\rho_o\dot{\theta}_x=0$$

$$(K'GA(y'-\theta_x))-m\ddot{y}=0 \qquad \text{.... (2.10)}$$

$$(EI\,\theta_x')'+K'GA(y'-\theta_x)-I_D\ddot{\theta}_x+I_p\rho_o\dot{\theta}_y=0$$

$$EI\,\theta_y'\,\delta\theta_y\Big|_o^l=0\ ;\ K'GA(x'-\theta_y)\delta x\Big|_o^l=0$$

.... (2.11)

$$EI\,\theta_x'\,\delta\theta_x\Big|_o^l=0\ ;\ K'GA(y'-\theta_x)\delta y\Big|_o^l=0$$

.... (2.12)

Equations (2.9) are the governing differential equations in XS plane, Eqn. (2.10) in YS plane and Eqns. (2.11) and (2.12) are the corresponding boundary conditions. These equations can also be derived by Newton's method [4], (see Appendix II).

Multiplying Eqns. (2.10) by $i = \sqrt{-1}$, combining it with Eqns. (2.9) and introducing the expressions

$$z = x+iy \text{ and } \phi = \theta_y + i\theta_x \qquad \ldots. (2.13)$$

complex differential equations for isotropic shaft are obtained as

$$(K'GA(z' - \phi))' - m\ddot{z} = 0 \qquad \ldots. (2.14)$$

$$(EI\,\phi')' + K'GA(z' - \phi) - I_D\ddot{\phi} + iI_p\,\varrho_o\,\dot{\phi} = 0$$

and for isotropic boundaries the complex boundary conditions become

$$\begin{aligned} &EI\,\phi' = 0 \text{ or } \phi = 0 \quad \text{at } x = 0 \text{ and } 1 \\ &K'GA(z' - \phi) = 0 \text{ or, } z=0 \text{ at } x=0 \text{ and } 1 \end{aligned} \qquad \ldots. (2.15)$$

The two equations given above can be combined into a single fourth order differential equation as

$$EI\,z^{iv} - I_D\left(1 + \frac{E}{K'G}\right)\ddot{z}'' + i\,I_p\,\varrho_o\,\ddot{z}'' + m\ddot{z} + \frac{m\,I_D}{K'GA}\ddot{\ddot{z}} - i\frac{mI_p\,\varrho_o}{K'GA}\dot{\ddot{z}} = 0$$

$$\ldots. (2.16)$$

which is same as that given by [4].

If shear deformations are negligible, the above equation becomes,

$$EI\, z^{iv} - I_D\, \ddot{z}'' + i\, I_p\, \Omega_o \dot{z}'' + m\ddot{z} = 0 \qquad \ldots\ (2.17)$$

The second and third terms represent the rotatory inertia and gyroscopic actions respectively. The above equation is same as that given in[3,4]. .

2.1.1 Non dimensionalisation :

The governing differential equations (2.14) and (2.17) are non-dimensionalised using the following parameters.

$$Z = \frac{z}{l} \; ; \; S = \frac{s}{l} \; ; \; T = \frac{t}{T^*} \; ; \; \Omega = \Omega_o T^*$$

$$A_n = \frac{A}{A_o} \; ; I_n = \frac{I}{I_o} \; ; \; T^* = \sqrt{\frac{\rho A_o l^4}{EI_o}} \qquad \ldots\ (2.18)$$

Where A_o and I_o are the area and area moment of inertia in bending at S = 0.

Using these parameters, Eqns. (2.14) and (2.15) become

$$(A_n\,(Z' - \phi))' - A_n\, Mc\, Re^2\, \ddot{Z} = 0 \qquad \ldots\ (2.19)$$

$$(I_n\, \phi')' + \frac{1}{Mc\, Re^2} A_n\,(Z' - \phi) - In\, Re^2\, \ddot{\phi} + i\, 2I_n\, Re^2\, \Omega\, \dot{\phi} = 0$$

$$Mc\, Re^2\, I_n\, \phi' = 0 \quad \text{or} \quad \phi = 0$$

$$A_n(Z' - \phi) = 0 \quad \text{or} \quad Z = 0 \qquad \ldots\ (2.20)$$

where $Mc = \frac{E}{K'G}$ and $Re^2 = \frac{I_o}{A_o l^2}$ $\qquad \ldots\ (2.21)$

It may be noted that now prime ($'$) indicates differentiation with respect to S and dot (.) with respect to T.

For uniform shaft A_n and I_n are unity , and Eqns. (2.19) and (2.20) become

$$(Z' - \phi)' - Mc\, Re^2\, \ddot{Z} = 0$$

$$\phi'' - \frac{1}{McRe^2}(Z' - \phi) - Re^2\, \ddot{\phi} + i\, 2Re^2\, \Omega\, \dot{\phi} = 0 \qquad \ldots\ (2.22)$$

$$Mc\, Re^2\, \phi' = 0 \quad \text{or} \quad \phi = 0$$

$$(Z' - \phi) = 0 \quad \text{or} \quad Z = 0 \qquad \ldots\ (2.23)$$

Similarly Eqn. (2.17) becomes

$$Z^{IV} - Re^2\,(\ddot{Z}'' - 2i\,\Omega\,\dot{Z}'') + \ddot{Z} = 0 \qquad \ldots\ (2.24)$$

2.1.2. FEM Equations :

Equations (2.19) are partial differential equations. Their solution is obtained by the finite element method. This method leads to simultaneous ordinary differential equations which can be solved in a routine way.

Descretizing the domain (0,1) by number of finite elements of length h (Refer Fig. 2.2) the variation of ϕ and Z over a typical element can be approximated as

$$Z^{(e)} = a + bZ + \ldots\ldots = [\,N^Z\,]\{Z\}^{(ne)}$$

$$\phi^{(e)} = a' + b'\,\phi + \ldots\ldots = [\,N^{\phi}\,]\{\phi\}^{(ne)} \qquad \ldots\ (2.25)$$

where $[N^Z]$ and $[N^{\phi}]$ are the shape functions ; $\{Z\}^{(ne)}$ and $\{\phi\}^{(ne)}$ are the nodal parameters.

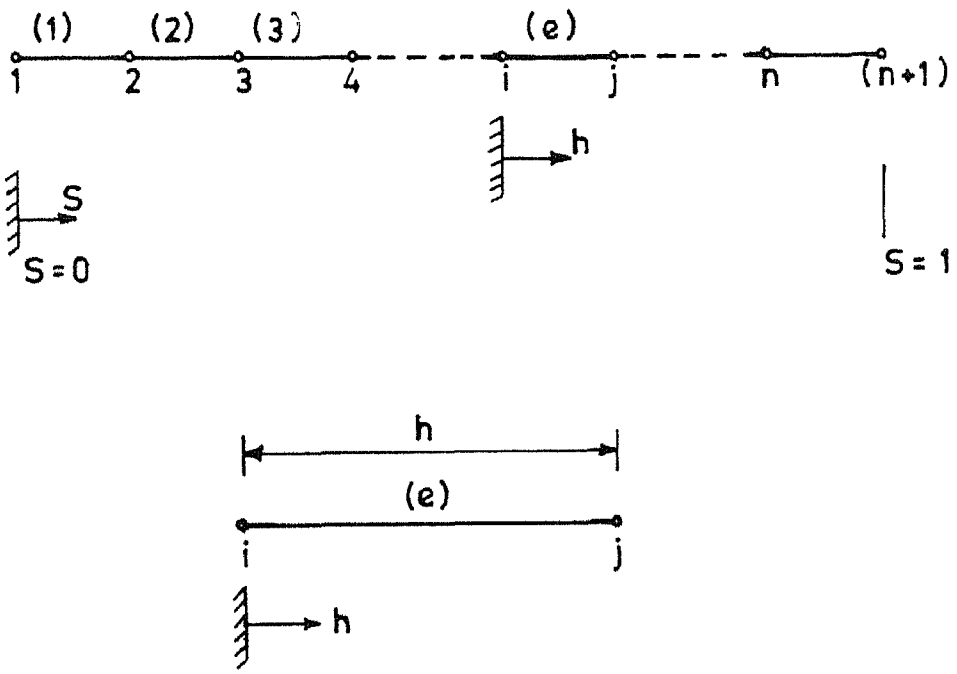

Fig. 2.2 Finite element discretization and typical element

Substituting Eqns. (2.25) in Eqns. (2.19), residues are obtained as

$$R^Z = (A_n\,(Z^{(e)\prime} - \phi^{(e)}))' - A_n\,Mc\,Re^2\,\ddot{Z}^{(e)}$$

$$R^\phi = (I_n\phi^{(e)\prime})' + \frac{1}{Mc\,Re^2}\,A_n(Z^{(e)\prime} - \phi^{(e)}) \quad \ldots\ (2.26)$$

$$I_n\,Re^2\,\ddot{\phi}^{(e)} + i\,2I_n\,Re^2\,\Omega\,\dot{\phi}^{(e)}$$

Minimising these residues by the Galerkin method, one gets after integration by parts,

$$\int_o^h N_i^{Z\prime} A_n(Z^{(e)\prime} - \phi^{(e)})\,dh + Mc\,Re^2 \int_o^h A_n\,N_i^Z\,\ddot{Z}^{(e)}\,dh$$

$$= N_i^Z\,A_n(Z^{(e)\prime} - \phi^{(e)})\Big|_o^h$$

$$\int_o^h N_i^{\phi\prime} I_n\,\phi^{(e)\prime}\,dh - \frac{1}{Mc\,Re^2} \int_o^h N_i^\phi\,A_n(Z^{(e)\prime} - \phi^{(e)})\,dh$$

$$+ Re^2 \int_o^h N_i^\phi\,I_n\,\ddot{\phi}^{(e)}\,dh - i2\,\Omega Re^2 \int_o^h N_i^\phi\,I_n\,\dot{\phi}^{(e)}\,dh$$

$$= N_i^\phi\,I_n\,\phi^{(e)\prime}\Big|_o^h$$

$\ldots\ (2.27)$

Watching the above equations, it is seen that compatibility of Z and ϕ at nodes and completeness of Z, Z', ϕ and ϕ' is required. A linear polynomial i.e. C_o element for Z and ϕ satisfies the above requirements, but it leads to ill-conditioning [16]. So a cubic polynomial i.e. C_1 element is chosen for

Z and ϕ both. With this, fewer elements need be used for same accuracy. Since $N^Z \equiv N^\phi$, the superscripts are dropped now onwards.

Substituting for $Z^{(e)}$ and $\phi^{(e)}$ and arranging Eqns. (2.27) in matrix form, one gets

$$\int_0^h A_n \{N'\} [N'] dh \{Z\}^{(ne)} - \int_0^h A_n \{N'\} [N] dh \{\phi\}^{(ne)}$$

$$+ Mc\, Re^2 \int_0^h A_n \{N\} [N] dh \{\ddot{Z}\}^{(ne)} = \{N\} A_n (Z^{(e)\prime} - \phi^{(e)}) \Big|_0^h \quad \text{and}$$

$$Mc\, Re^2 \int_0^h I_n \{N'\} [N'] dh \{\phi\}^{(ne)} - \int_0^h A_n \{N\} [N'] dh \{Z\}^{(ne)}$$

$$+ \int_0^h A_n \{N\} [N] dh \{\phi\}^{(ne)} + Mc\, Re^4 \int_0^h I_n \{N\} [N] dh \{\ddot{\phi}\}^{(ne)}$$

$$- 2i\, Mc\, Re^4 \int_0^h I_n \{N\} [N] dh \{\dot{\phi}\}^{(ne)} = \{N\} Mc\, Re^2\, In\, \phi' \Big|_0^h$$

.... (2.28)

These equation can be arranged in the form

$$\begin{bmatrix} McRe^2[MA]^{(e)} & [0] \\ [0] & McRe^4[MI]^{(e)} \end{bmatrix} \begin{bmatrix} \{\ddot{Z}\}^{(ne)} \\ \{\ddot{\phi}\}^{(ne)} \end{bmatrix} - i\Omega \begin{bmatrix} [0] & [0] \\ [0] & 2McRe^4[MI]^{(e)} \end{bmatrix} \begin{bmatrix} \{\dot{Z}\}^{(ne)} \\ \{\dot{\phi}\}^{(ne)} \end{bmatrix}$$

$$+ \begin{bmatrix} [KA]^{(e)} & -[KU]^{(e)} \\ -[KU]^{(e)^T} & McRe^2[KA]^{(e)} + [MA]^{(e)} \end{bmatrix} \begin{bmatrix} \{Z\}^{(ne)} \\ \{\phi\}^{(ne)} \end{bmatrix} = \begin{bmatrix} \{FBS\}^{(ne)} \\ \{FBM\}^{(ne)} \end{bmatrix}$$

or $[M]^{(e)} \{\ddot{q}\}^{(ne)} - i\Omega [G]^{(e)} \{\dot{q}\}^{(ne)} + [K]^{(e)} \{q\}^{(ne)} = \{FB\}^{(ne)}$

.... (2.29)

where

$$[KA]^{(e)} = \int_o^h A_n \{N'\} \lfloor N' \rfloor \, dh$$

$$[KU]^{(e)} = \int_o^h A_n \{N'\} \lfloor N \rfloor \, dh$$

$$[KI]^{(e)} = \int_o^h I_n \{N'\} \lfloor N' \rfloor \, dh$$

$$[MA]^{(e)} = \int_o^h A_n \{N\} \lfloor N \rfloor \, dh$$

$$[MI]^{(e)} = \int_o^h I_n \{N\} \lfloor N \rfloor \, dh$$

$$\{FBS\}^{(ne)} = \begin{Bmatrix} -A_n (Z^{(e)\prime} - \phi) \Big|_j \\ 0 \\ A_n (Z^{(e)\prime} - \phi) \Big|_k \\ 0 \end{Bmatrix} \qquad \ldots\ (2.30)$$

$$\{FBI\}^{(ne)} = \begin{Bmatrix} -McRe^2 \; In \; \phi' \Big|_j \\ 0 \\ McRe^2 \; I_n \; \phi' \Big|_k \\ 0 \end{Bmatrix}$$

It may be noted that here all matrices $[M]^{(e)}$, $[G]^{(e)}$ and $[K]^{(e)}$ are symmetric.

Equation (2.24) is the governing equation when shear deformation is negligible. This is a single fourth order differential equation. Its FEM equations are obtained in the routine way and are

$$[M]^{(e)}\{\ddot{q}\}^{(ne)} - i\Omega[G]^{(e)}\{\dot{q}\}^{(ne)} + [K]^{(e)}\{q\}^{(ne)} = \{FB\}^{(ne)} \quad \ldots\ldots (2.31)$$

where,

$$[M]^{(e)} = \int_0^h \{N\}[N]\,dh + Re^2 \int_0^h \{N'\}[N']dh$$

is the elemental mass matrix,

$$[G]^{(e)} = 2Re^2 \int_0^h \{N'\}[N']dh$$

is the elemental gyroscopic matrix,

$$[K]^{(e)} = \int_0^h \{N''\}[N'']dh$$

is the elemental stiffness matrix,

$$\{q\}^{(ne)} = \{Z\}^{(ne)}$$

is the elemental nodal displacement vector

and

$$\{FB\}^{(ne)} = -\{N\}Z^{(e)'''}\Big|_0^h + \{N'\}Z^{(e)''}\Big|_0^h + \{N\}Re^2\ \ddot{Z}'\Big|_0^h - \{N\}2Re^2\,\Omega\,\dot{Z}'\Big|_0^h$$

is the elemental nodal force vector.

It may be noted that here C_1 element is needed, and all matrices are symmetric.

2.2 DUAL SHAFT :

Non-circular shafts or circular shafts with key ways and slots will have different stiffnesses in different directions. Stiffness in any direction can be determined, once stiffnesses in two principal directions are known. Thus if I_1

and I_2 are the principal moments of inertia in principal directions I and II, then moments of inertia in X and Y direction are, Fig.(2.3 a), [17] .

$$I_{xx} = \left(\frac{I_1+I_2}{2}\right) + \left(\frac{I_1-I_2}{2}\right)\cos 2\Psi$$

$$I_{yy} = \left(\frac{I_1+I_2}{2}\right) - \left(\frac{I_1-I_2}{2}\right)\cos 2\Psi \qquad \ldots\ (2.32)$$

$$I_{xy} = \left(\frac{I_1-I_2}{2}\right) \sin 2\Psi$$

Such shafts are referred as dual shafts in literature. For such shafts the moment curvature relations are [18]

$$M_x = -\left[EI_{xx}\,\theta_x' + EI_{xy}\,\theta_y'\right]$$

$$\ldots\ (2.33)$$

$$M_y = \left[EI_{yy}\,\theta_y' + EI_{xy}\,\theta_x'\right]$$

Shaft is rotating with angular velocity Ω_o. X and Y are the fixed axes i.e. they do not change. At any time the principal axes make an angle $\Omega_o t$ with X,Y-axes Fig. 2.3(b).

Using the Eqns. (2.32) ($\Psi = -\Omega_o t$) and (2.33) and following the procedure of Appendix II, the equations of motion for uniform dual shaft become,

For bending in XS plane :

$$K'GA\,(x' - \theta_y)' - m\ddot{x} = 0$$

$$\ldots\ (2.34)$$

$$E\left(\frac{I_1+I_2}{2} - \frac{I_1-I_2}{2}\cos 2\,\Omega_o t\right)\theta_y'' - E\left(\frac{I_1-I_2}{2}\sin 2\,\Omega_o t\right)\theta_x''$$

$$+ K'GA(x' - \theta_y) - I_D\,\ddot{\theta}_y - I_D\,\Omega_o\,\dot{\theta}_x = 0$$

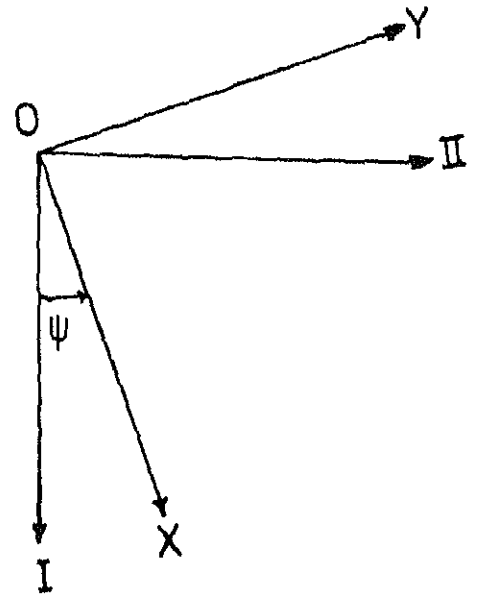

(a)

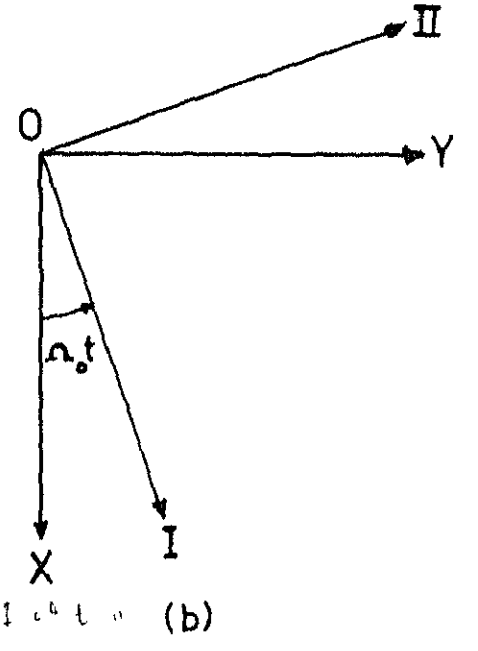

(b)

Fig: 2.3 (a) Position of frame (XYS) relative to (IIS)
(b) Position of frame (IIS) relative to (XYS)

For bending in YS plane :

$$K'GA\,(y' - \theta_x)' - m\ddot{y} = 0$$

$$E\left(\frac{I_1+I_2}{2} + \frac{I_1-I_2}{2}\cos 2\,\Omega_o t\right)\theta_x'' - E\left(\frac{I_1-I_2}{2}\sin 2\,\Omega_o t\right)\theta_y'' \qquad \ldots\ (2.35)$$

$$+ K'GA\,(y'-\theta_x) - I_D\,\ddot{\theta}_x + I_p\,\Omega_o\,\dot{\theta}_y = 0$$

Multiplying Eqn. (2.35) with $i = \sqrt{-1}$ and combining with Eqn. (2.34), using the notations $z = x+iy$; $\theta = \theta_y + i\theta_x$ and $\bar{\theta} = \theta_y - i\theta_x$, the equations of motion become

$$K'GA\,(z' - \theta)' - m\ddot{z} = 0$$

$$E\left(\frac{I_1+I_2}{2}\right)\theta'' - E\left(\frac{I_1-I_2}{2}\right)\cos 2\,\Omega_o t\,\bar{\theta}''$$

$$-iE\left(\frac{I_1-I_2}{2}\right)\sin 2\,\Omega_o t\,\bar{\theta}'' + K'GA\,(z'-\theta) \qquad \ldots\ (2.36)$$

$$- I_D\,\ddot{\theta} + iI_p\,\Omega_o\dot{\theta} = 0$$

Combining second and third terms of second equation, one gets

$$K'GA\,(z' - \theta)' - m\ddot{z} = 0$$

$$E\left(\frac{I_1+I_2}{2}\right)\theta'' - E\left(\frac{I_1-I_2}{2}\right)\bar{\theta}''e^{i2\,\Omega_o t} + K'GA\,(z' - \theta) \qquad \ldots\ (2.37)$$

$$- I_D\,\ddot{\theta} + iI_p\,\Omega_o\dot{\theta} = 0$$

Multiplying Eqn. (2.37) by $e^{-i\,\Omega_o t}$

$$K'GA\,(z' - \theta)'\,e^{-i\,\Omega_o t} - m\ddot{z}\,e^{-i\,\Omega_o t} = 0$$

$$E\left(\frac{I_1+I_2}{2}\right)\theta''e^{-i\,\Omega_o t} - E\left(\frac{I_1-I_2}{2}\right)\bar{\theta}''\,e^{i\,\Omega_o t} + K'GA(z' - \theta)e^{-i\,\Omega_o t} \qquad \ldots(2.38)$$

$$-I_D\,\ddot{\theta}\,e^{-i\,\Omega_o t} + iI_p\,\Omega_o\,\dot{\theta}\,e^{-i\,\Omega_o t} = 0$$

Equations (2.38) have coefficients which are functions of time. This time dependence can be eliminated by defining

$$\zeta = z\, e^{-i\,\Omega_o t} \; ; \; \phi = \theta e^{-i\,\Omega_o t} \; ; \; \bar{\phi} = \bar{\theta}\, e^{i\,\Omega_o t} \qquad \ldots\ (2.39)$$

Thus Eqns. (2.38) become

$$K'GA\,(\zeta' - \phi)' - m\ddot{\zeta} - i2m\,\Omega_o\dot{\zeta} + m\Omega_o^2\zeta = 0$$

$$E\left(\frac{I_1+I_2}{2}\right)\phi'' - E\left(\frac{I_1-I_2}{2}\right)\bar{\phi}'' + K'GA\,(\zeta' - \phi) \qquad \ldots\ (2.40)$$

$$-I_D\,\ddot{\phi} - i2I_D\,\Omega_o\dot{\phi} + I_D\,\Omega_o^2\,\phi$$

$$+ iI_p\,\Omega_o\dot{\phi} - I_p\,\Omega_o^2\,\phi = 0$$

Taking $I_D = \frac{1}{2} I_p$, as done in [4], the above equations become

$$K'GA(\zeta' - \phi)' - m\ddot{\zeta} - i2m\,\Omega_o\dot{\zeta} + m\,\Omega_o^2\zeta = 0$$

$$E\left(\frac{I_1+I_2}{2}\right)\phi'' - E\left(\frac{I_1-I_2}{2}\right)\bar{\phi}'' + K'GA(\zeta' - \phi) \qquad \ldots\ (2.41)$$

$$- I_D\,\ddot{\phi} - I_D\,\Omega_o^2\,\phi = 0$$

These are differential equations in complex variables

$$\zeta = \xi_o + i\eta_o \; ; \; \phi = \theta_\eta + i\theta_\xi \; , \; \bar{\phi} = \theta_\eta - i\theta_\xi \qquad \ldots\ (2.42)$$

where ξ_o, η_o are the deflections along I and II respectively and θ_η, θ_ξ are the bending slopes in IS plane and IIS plane respectively.

Separating real and imaginary parts, one gets

$$K'GA(\xi_o' - \theta_\eta)' - m\xi_o + 2m\Omega_o\dot{\eta}_o + m\Omega_o^2\xi_o = 0$$

$$EI_2\,\theta_\eta'' + K'GA(\xi_o' - \theta_\eta) - I_D\ddot{\theta}_\eta - I_D\Omega_o^2\theta_\eta = 0 \qquad \ldots\ (2.43)$$

$$K'GA(\dot{\eta}_o - \theta_\xi)' - m\ddot{\eta}_o - 2m\Omega_o\xi_o + m\Omega_o^2\eta_o = 0$$

$$EI_1\,\theta_\xi'' + K'GA(\eta_o' - \theta_\xi) - I_D\ddot{\theta}_\xi - I_D\Omega_o^2\theta_\xi = 0 \qquad \ldots\ (2.44)$$

Equations (2.43) correspond to IS plane and Eqns. (2.44) correspond to IIS plane.

It may be noted that Eqns. (2.43) and (2.44) differ from those given by Dimentberg [4] . It is because of the definitions of I_1 and I_2, which differ from Dimentberg's definition.

By observing Eqns. (2.39), it may also be noted that, the natural frequencies obtained using these conversions, will be the natural frequencies (λ') in I II S frame. To obtain the natural frequencies (λ) in XYS frame, the following relation is to be used.

$$\lambda = \lambda' + \Omega_o \qquad \ldots\ (2.45)$$

Two second order equations of Eqn. (2.43) can be combined into a fourth order equation and same can be done for Eqn. (2.44). These two fourth order equations are same as

those given by Dimentberg [4] ; which were obtained in a direct way without deriving the second order equations. These second order equations are of great advantage in FEM formulation, as all boundary conditions (geometrical and natural) can be incorporated exactly. When shear deformations are negligible, these two fourth order equations become for bending in IS plane,

$$EI_2\ \xi_o^{iv} - I_D(\ddot{\xi}_o'' + \Omega_o^2\ \xi_o'') + m(\xi_o - 2\ \Omega_o\dot{\eta}_o - \Omega_o^2\ \xi_o) = 0 \qquad \ldots\ (2.46)$$

and for bending in IIS plane

$$EI_1\ \eta_o^{iv} - I_D(\ddot{\eta}_o'' + \Omega_o^2\eta_o'') + m\ (\ddot{\eta}_o + 2\ \Omega_o\ \dot{\xi}_o - \Omega_o^2\ \eta_o) = 0 \qquad \ldots\ (2.47)$$

2.2.1 Non-dimensionalisation :

The non-dimensional parameters used are

$$\xi = \frac{\xi_o}{l}\ ;\ \eta = \frac{\eta_o}{l}\ ;\ S = \frac{s}{l}\ ;\ T = \frac{t}{T^*}\ ;$$
$$\Omega = \Omega_o T^*;\ T^* = \sqrt{\frac{\rho A l^4}{EI_1}}\ ;\ C = \frac{I_1}{I_2}\ ;\ C_d = \frac{k^2}{k_1^2} \qquad \ldots\ (2.48)$$

where k is the radius of gyration for mass moment of inertia and k_1 is the radius of gyration for area moment of inertia I_1. With these the non-dimensional form of Eqns. (2.43) and (2.44) are

$$(\xi' - \theta_\eta)' - Mc\ Re_1^2\ (\xi - 2\Omega\dot{\eta} - \Omega^2\xi) = 0$$

$$\frac{McRe_1^2}{C}\ \theta_\eta'' + (\xi' - \theta_\eta) - C_d\ Mc\ Re_1^4(\ddot{\theta}_\eta + \Omega^2\ \theta_\eta) = 0 \qquad \ldots\ (2.49)$$

and

$$(\eta' - \theta\xi)' - Mc\ Re_1^2(\ddot{\eta} + 2\ \Omega - \xi\Omega^2\eta) = 0$$

$$Mc\ Re_1^2\ \theta_\xi'' + (\eta' - \theta_\xi) - C_d\ Mc\ Re_1^4\ (\ddot{\theta}_\xi + \Omega^2\theta_\xi) = 0 \qquad \ldots\ (2.50)$$

where $Re_1^2 = \frac{I_1}{Al^2}$, is the rotatory inertia coefficient and, $Mc = \frac{E}{K'G}$ is the material constant.

Similarly Eqns. (2.46) and (2.47) become

$$\xi^{IV} - C\ C_d Re_1^2\ (\xi'' + \Omega^2\xi'') + C\ (\ddot{\xi} - 2\Omega\dot{\eta} - \Omega^2\xi) = 0 \qquad \ldots\ (2.51)$$

and

$$\eta^{IV} - C_d\ Re_1^2\ (\ddot{\eta}'' + \Omega^2\ \eta'') + (\ddot{\eta} + 2\ \Omega\dot{\xi} - \Omega^2\eta) = 0 \qquad \ldots\ (2.52)$$

2.2.2 FEM Equations:

Proceeding as in section (2.1.2) finite element equations for dual shaft are

$$[M]^{(e)}\ \{\ddot{q}\}^{(ne)} + [G]^{(e)}\ \{\dot{q}\}^{(ne)} + [K]^{(e)}\ \{q\}^{(ne)} = \{FB\}^{(ne)} \qquad \ldots\ (2.53)$$

Where

$$[M^{(e)}] = \begin{bmatrix} Mc\ Re_1^2[M_1] & [0] & [0] & [0] \\ [0] & C_d Mc\ Re_1^4 [M_1] & [0] & [0] \\ [0] & [0] & Mc\ Re_1^2[M_1] & [0] \\ [0] & [0] & [0] & C_d Mc\ Re_1^4 [M_1] \end{bmatrix}$$

is the elemental mass matrix ,

$$[G^{(e)}] = \begin{bmatrix} [0] & [0] & -2\ \Omega McRe_1^2[M_1] & [0] \\ [0] & [0] & [0] & [0] \\ 2\ \Omega McRe_1^2[M_1] & [0] & [0] & [0] \\ [0] & [0] & [0] & [0] \end{bmatrix}$$

is the elemental gyroscopic matrix,

$$[K^{(e)}] = \begin{bmatrix} ([K_1]-McRe_1^2\ \Omega^2[M_1]) & [K_2] & [0] & [0] \\ & (\frac{McRe_1^2}{C}[K_1] & [0] & [0] \\ & +(1+C_d McRe_1^4\ \Omega^2) & & \\ & [M_1]) & & \\ \text{Sym.} & & K_1 - McRe_1^2\ \Omega^2 & [K_2] \\ & & [M_1] & \\ & & & (McRe_1^2\ [K_1] \\ & & & +(1+C_d McRe_1^4 \\ & & & .\ \Omega^2)\ [M_1]) \end{bmatrix}$$

is the elemental stiffness matrix,

$$\{q\}^{(ne)} = \begin{bmatrix} \{\xi\}^{(ne)} \\ \{\theta_\eta\}^{(ne)} \\ \{\eta\}^{(ne)} \\ \{\theta_\xi\}^{(ne)} \end{bmatrix}$$

is the nodal displacement vector of the element,

$$\{FB\}^{(ne)} = \begin{bmatrix} \{N\}\,(\{\xi\}^{(e)\prime} - \theta_\eta^{(e)})\,\Big|_o^h \\ \frac{McRe_1^2}{C}\,\{N\}\,\theta_\eta^{(e)\prime}\,\Big|_o^h \\ \{N\}\,(\eta^{(e)\prime} - \theta_\xi^{(e)})\,\Big|_o^h \\ McRe_1^2\,\{N\}\,\theta_\xi^{(e)\prime}\,\Big|_o^h \end{bmatrix}$$

is the nodal force vector of the element,

and

$$[M_1] = \int_o^h \{N\}\,[N]\,dh$$

$$[K_1] = \int_o^h \{N'\}\,[N']\,dh \qquad \ldots\ (2.54)$$

$$[K_2] = -\int_o^h \{N'\}\,[N]\,dh$$

Here $[M]^{(e)}$ and $[K]^{(e)}$ are symmetric matrices, and $[G]^{(e)}$ is skew-symmetric matrix.

Similarly FEM equations for a dual shaft without shear, Eqns. (2.51) and (2.52), become

$$[M]^{(e)}\{\ddot{q}\}^{(ne)} + \Omega[G]^{(e)}\{\dot{q}\}^{(ne)} + [K]^{(e)}\{q\}^{(ne)} = \{FB\}^{(ne)} \quad \ldots\ldots (2.55)$$

where,

$$[M]^{(e)} = \begin{bmatrix} C([M_1] + C_d Re_1^2 [K_1]) & [0] \\ [0] & ([M_1] + C_d Re_1^2 [K_1]) \end{bmatrix},$$

is the elemental mass matrix,

$$[G]^{(e)} = \begin{bmatrix} [0] & -2C[M_1] \\ 2[M_1] & [0] \end{bmatrix}$$

is the elemental gyroscopic matrix ,

$$[K]^{(e)} = \begin{bmatrix} [K_2] + C\Omega^2(C_d Re_1^2 [K_1] - [M_1]) & 0 \\ [0] & [K_2] + \Omega^2(C_d Re_1^2 [K_1] - [M_1]) \end{bmatrix}$$

is the elemental stiffness matrix,

$$\{FB\}^{(ne)} \begin{bmatrix} -\{N\}\xi^{(e)'''}\Big|_0^h + \{N'\}\xi^{(e)''}\Big|_0^h + CC_d Re_1^2\{N\}\xi^{(e)'}\Big|_0^h + CC_d Re_1^2\Omega^2\{N\}\xi^{(e)}\Big|_0^h \\ -\{N\}\eta^{(e)'''}\Big|_0^h + \{N'\}\eta^{(e)''}\Big|_0^h + C_d Re_1^2\{N\}\ddot{\eta}^{(e)}\Big|_0^h + C_d Re_1^2\Omega^2\{N\}\eta^{(e)'}\Big|_0^h \end{bmatrix}$$

is the elemental nodal force vector,

$$\{q\}^{(ne)} = \begin{bmatrix} \{\xi\}^{(ne)} \\ \{\eta\}^{(ne)} \end{bmatrix}$$

is the elemental nodal displacement vector

and

$$[K_1] = \int_0^h \{N\}\,[N]\,dh$$

$$[K_1] = \int_0^h \{N'\}\,[N']\,dh \qquad \ldots\ (2.56)$$

$$[K_2] = \int_0^h \{N''\}\,[N'']\,dh$$

For both the cases C_1 element has been used as discussed in section (2.1). Here $[M]^{(e)}$ and $[K]^{(e)}$ are symmetric matrices, and $[G]^{(e)}$ is unsymmetric matrix.

2.3 ISOTROPIC SHAFT WITH DAMPING :

The friction offers resistance to motion and this usually leads to damping of natural vibrations. The friction arising between rotating and stationary parts, such as bearings is called as external friction and damping arising due to this is called external damping. The friction arising within the rotating shaft due to resistance of the particles of material is called internal friction and the damping due to this is called as internal damping.

External damping can be incorporated by modelling the bearing as dash-pot model with a viscous damping coefficient C

and equating the shear force to the damping force, while applying the boundary conditions.

To take internal damping into account, two forms of damping models are taken. In the first, it is linear velocity dependent viscous model, for which the constitutive relation relating the axial stress σ_s to the axial strain ε_s is [9] .

$$\sigma_s = \eta_v E \dot{\varepsilon}_s \qquad \ldots. (2.57)$$

where η_v is viscous damping coefficient.

The other model is frequency independent hysteretic damping which is expressed by the loss factor η_H which is related to loss angle γ_H [19] by

$$\tan \gamma_H = \eta_H \qquad \ldots. (2.58)$$

The constitutive relation for this case is [9]

$$\sigma_s = E \left[\left(\frac{1}{\sqrt{1+\eta_H^2}}\right)\varepsilon_s + \left(\frac{\eta_H}{\lambda\sqrt{1+\eta_H^2}}\right)\dot{\varepsilon}_s \right] \qquad \ldots. (2.59)$$

Combining the two models, Eqn. (2.57) and Eqn. (2.59) one gets

$$\sigma_s = E \left[\left(\frac{1}{\sqrt{1+\eta_H^2}}\right)\varepsilon_s + \left(\eta_v + \frac{\eta_H}{\lambda\sqrt{1+\eta_H^2}}\right)\dot{\varepsilon}_s \right] \qquad \ldots. (2.60)$$

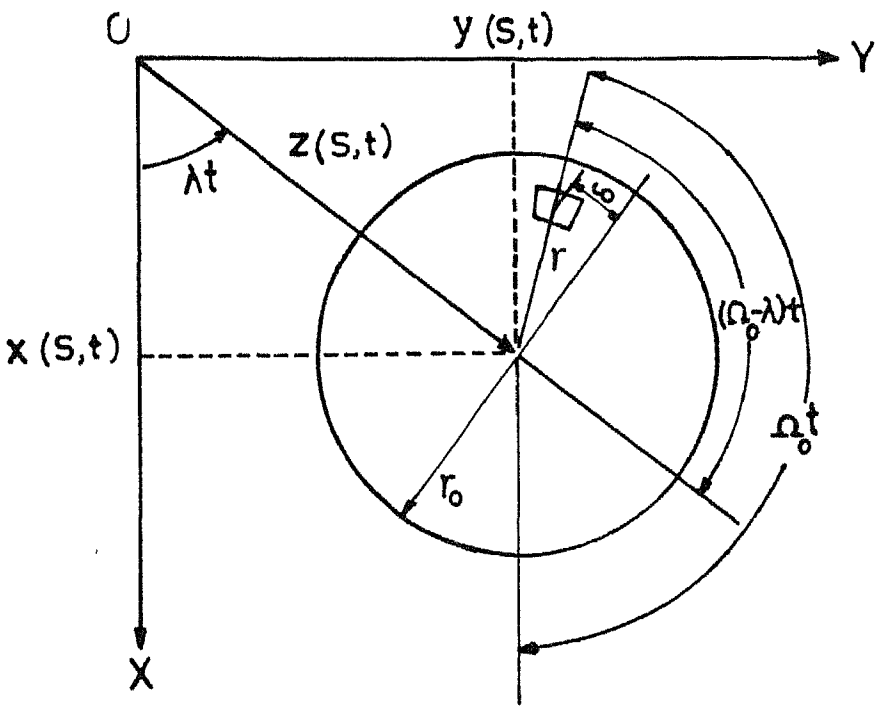

Fig: 2.4 Shaft cross section in deflected position.

Referring to Fig.(2.4), $z(s,t)$ is the distance of neutral axis of cross section, λ is the speed of precession, Ω_o is the spin speed. The normal strain in the differential area dA, at a radius r, is

$$\varepsilon_s = -\frac{\delta}{\rho_c} = -r\cos(\Omega-\lambda)t\,\frac{\partial^2 z}{\partial s^2} \qquad \ldots\ (2.61)$$

where δ is the perpendicular distance of dA from neutral axis. From Fig. (2.4), moments about X and Y axes are

$$M_x = \int_0^{2\pi}\int_0^{r_o}[y + r\sin\Omega t\,]\,\sigma_s\ dA$$

$$M_y = -\int_0^{2\pi}\int_0^{r_o}[x + r\cos\Omega t\,]\,\sigma_s\ dA \qquad \ldots\ (2.62)$$

Using Eqns. (2.60) and (2.61), moments from Eqn. (2.62) become [9],

$$\begin{bmatrix} M_x \\ M_y \end{bmatrix} = EI\begin{bmatrix} -\left(\frac{1+\eta_H}{\sqrt{1+\eta_H^2}}\right) & \left(\Omega_o\eta_V + \frac{\eta_H}{\sqrt{1+\eta_H^2}}\right) \\ \left(\Omega_o\eta_V + \frac{\eta_H}{\sqrt{1+\eta_H^2}}\right) & \left(\frac{1+\eta_H}{\sqrt{1+\eta_H^2}}\right) \end{bmatrix}\begin{bmatrix} y'' \\ x'' \end{bmatrix}$$

$$+ EI\begin{bmatrix} -\eta_V & 0 \\ 0 & \eta_V \end{bmatrix}\begin{bmatrix} \dot{y}'' \\ \dot{x}'' \end{bmatrix} \qquad \ldots\ (2.63)$$

Using the above Eqn. (2.63) in Eqns. (A 2.3) and (A 2.4) of Appendix II, the governing differential equations are obtained as,

$$EI\left[\frac{1+\eta_H}{\sqrt{1+\eta_H^2}}\,x^{iv} + \left(\frac{\eta_H}{\sqrt{1+\eta_H^2}} + \eta_V\ \Omega_o\right) y^{iv} + \eta_V\ \dot{x}^{iv}\right] - I_D\ddot{x}'' - I_p\,\Omega_o\dot{y}'' + m\ddot{x} = 0 \qquad \ldots\ (2.64)$$

for bending in XS plane and

$$EI\left[\frac{1+\eta_H}{\sqrt{1+\eta_H^2}}\,y^{iv} - \left(\frac{\eta_H}{\sqrt{1+\eta_H^2}} + \eta_V\ \Omega_o\right) x^{iv} + \eta_V\ \dot{y}^{iv}\right] - I_D\ddot{y}'' + I_p\,\Omega_o\,\dot{x}'' + m\ddot{y} = 0$$

for bending in YS plane.

2.3.1 Non-dimensionalisation :

The non-dimensional form of Eqns. (2.64), are obtained following the procedure of section (2.1.1). The non-dimensional parameters used are,

$$X = \frac{x}{l}\ ;\ Y = \frac{y}{l}\ ;\ T = \frac{t}{T^*}\ ;\ \Omega = \Omega_o T^*$$

$$\eta_{VN} = \frac{\eta_V}{T^*}\ ;\ T^* = \sqrt{\frac{\rho A l^4}{EI}} \qquad \ldots\ (2.65)$$

$$K_{xx} = \frac{k_{xx} l^3}{EI}\ ,\ C_{xx} = \frac{c_{xx} l^3}{EI\ T^*}$$

Then, Eqns. (2.64) in the non-dimensional form, are

$$\left(\frac{1+\eta_H}{\sqrt{1+\eta_H^2}}\right) X^{IV} + \left(\frac{\eta_H}{\sqrt{1+\eta_H^2}} + \eta_{VN}\ \Omega\right) Y^{IV} + \eta_{VN}\ \dot{X}^{IV} - Re^2\,(\dot{X}'' + 2\,\Omega\,\dot{Y}'') + \ddot{X} = 0$$

$$\left(\frac{1+\eta_H}{\sqrt{1+\eta_H^2}}\right) Y^{IV} - \left(\frac{\eta_H}{\sqrt{1+\eta_H^2}} + \eta_{VN}\Omega\right) X^{IV} + \eta_{V} \dot{Y}^{IV}$$

$$- Re^2 \left(\ddot{Y}'' - 2\ \Omega \dot{X}''\right) + \ddot{Y} = 0 \qquad \ldots\ (2.66)$$

where $Re^2 = \frac{I}{Al^2}$

2.3.2 FE. Equations :

Following a procedure similar to the one explained in section (2.1.2) in detail, FEM equations are obtained and expressed in matrix form as follows.

$$[M]^{(e)} \{\ddot{q}\}^{(ne)} + [C]^{(e)} \{\dot{q}\}^{(ne)} + [K]^{(e)} \{q\}^{(ne)} = \{FB\}^{(ne)} \qquad \ldots\ (2.67)$$

where

$$[M]^{(e)} = \begin{bmatrix} [M_1] + Re^2\ [K_1] & [0] \\ [0] & [M_1] + Re^2\ [K_1] \end{bmatrix}$$

is the elemental mass matrix,

$$[C]^{(e)} = \begin{bmatrix} \eta_V\ [K_2] & 2\ \Omega Re^2\ [K_1] \\ -2\ \Omega Re^2\ [K_1] & \eta_V\ [K_2] \end{bmatrix}$$

is the elemental damping matrix,

$$[K]^{(e)} = \begin{bmatrix} \left(\frac{1+\eta_H}{\sqrt{1+\eta_H^2}}\right)\ [K_2] & \left(\frac{\eta_H}{\sqrt{1+\eta_H^2}} + \eta_{VN}\Omega\right)\ [K_2] \\ -\left(\frac{\eta_H}{\sqrt{1+\eta_H^2}} + \eta_{VN}\Omega\right)[K_2] & \left(\frac{1+\eta_H}{\sqrt{1+\eta_H^2}}\right)\ [K_2] \end{bmatrix}$$

is the elemental stiffness matrix,

$$\{q\}^{(ne)} \quad \begin{bmatrix} \{X\}^{(ne)} \\ \{Y\}^{(ne)} \end{bmatrix}$$

is the nodal displacement vector of the element,

$$\{FB\}^{(ne)} \quad \begin{bmatrix} \{F_1\}^{(ne)} \\ \{F_2\}^{(ne)} \end{bmatrix}$$

is the nodal force vector of the element,

where

$$\{F_1\}^{(ne)} = \left(\frac{1+\eta_H}{\sqrt{1+\eta_H^2}}\right)\left[-\{N\}\,X^{(e)'''}\Big|_o^h + \{N'\}\,X^{(e)''}\Big|_o^h\right]$$

$$+\left(\frac{\eta_H}{\sqrt{1+\eta_H^2}} + \eta_{VN}\,\Omega\right)\left[-\{N\}\,Y^{(e)'''}\Big|_o^h + \{N'\}\,Y^{(e)''}\Big|_o^h\right]$$

$$+\,\eta_{VN}\left[-\{N\}\,\dot{X}^{(e)'''}\Big|_o^h + \{N'\}\,\dot{X}^{(e)''}\Big|_o^h\right]$$

$$+\,Re^2\left[\{N\}\,\ddot{X}^{(e)'}\Big|_o^h + \{N\}\,\dot{Y}^{(e)'}\Big|_o^h\right].$$

$$\{F_2\}^{(ne)} = \left(\frac{1+\eta_H}{\sqrt{1+\eta_H^2}}\right)\left[-\{N\}\,Y^{(e)'''}\Big|_o^h + \{N'\}\,Y^{(e)''}\Big|_o^h\right]$$

$$-\left(\frac{\eta_H}{\sqrt{1+\eta_H^2}} + \eta_{VN}\right)\left[-\{N\}\,\dot{Y}^{(e)'''}\Big|_o^h + \{N'\}\,\dot{Y}^{(e)''}\Big|_o^h\right]$$

$$+\eta_{VN}\left[-\{N\}\,\dot{Y}^{(e)'''}\Big|_o^h + \{N'\}\,\dot{Y}^{(e)''}\Big|_o^h\right]$$

$$+\,Re^2\left[\{N\}\,\ddot{Y}^{(e)'}\Big|_o^h - \{N\}\,\dot{Y}^{(e)'}\Big|_o^h\right]$$

and

$$[M_1] = \int_0^h \{N\}[N]dh$$

$$[K_1] = \int_0^h \{N'\}[N']dh \qquad (2.68)$$

$$[K_2] = \int_0^h \{N''\}[N'']dh$$

Here also C_1 element has been used Matrix $[M]^{(e)}$ is symmetric and matrices $[C]^{(e)}$ and $[K]^{(e)}$ are skew-symmetric.

CHAPTER - III

RESULTS AND DISCUSSION

Computer programs in FORTRAN IV have been developed to determine the natural frequencies and critical speeds, for all the cases of shafts, formulated in Chapter 2.

3.1 METHOD OF SOLUTION :

Element matrices, $[M]^{(e)}$, $[G]^{(e)}$, $[C]^{(e)}$ and, $[K]^{(e)}$, were calculated using Gauss quadrature with four Gauss points. These matrices are assembled in the usual way and boundary conditions applied.

3.1.1 Isotropic shaft without damping :

Assuming a hormonic solution of the form

$$\{q\}^n = \{q_o\}^n e^{i\lambda t} \qquad \ldots\ (3.1)$$

and applying to the assembled form of Eqn. (2.29) the following equation is obtained

$$(-\lambda^2 [M] + \Omega\lambda [G] + [K])\{q_o\}^{(n)} = 0 \qquad \ldots\ (3.2)$$

For critical speeds in forward precession, the critarion is

$$\lambda = \Omega \qquad \ldots\ (3.3)$$

and for backward precession it is $\lambda = -\Omega$.

Applying these critaria., Eqn. (3.2) becomes

$$[K]\{q\}_o^n = \Omega^2 ([M] \mp [G]) \{q\}_o^n \qquad \ldots\ (3.4)$$

where minus sign is to be used for forward precession and plus sign for backward precession. The eigenvalues Ω are the critical speeds. The above eigenvalue problem is solved using NAG library subroutine F02AEF.

3.1.2 Dual shaft without damping :

The method of solution for determining the critical speeds of dual shaft is given in this section. Governing differential equations for this case are in reference frame I IIS . The natural frequencies (λ') in this frame of reference are related to natural frequencies (λ) in frame of reference XYS , by Eqn. (2.45). It is to be noted herethat in the Eqn. (2.45) Ω_o is the spin speed in dimensional form, which is later non dimensionalised as Ω.

Noting that, the critarion for critical speeds to occure in forward precession is $\lambda = \Omega$, in reference frame XYS , the critarion in I IIS frame becomes

$$\lambda' = 0 \qquad \ldots\ (3.5)$$

Considering a dual shaft without shear, Eqn. (2.55), the $[K]^e$ matrix can be expressed in the following form.

$$[K]^{(e)} = [KD]^{(e)} - \Omega^2 [MD]^{(e)} \qquad \ldots\ (3.6)$$

Where

$$[KD]^{(e)} = \begin{bmatrix} [K_2] & [0] \\ [0] & [K_2] \end{bmatrix}$$

and

$$[MD]^{(e)} = \begin{bmatrix} C([M_1] - C_d\, Re_1^2 [K_1]) & [0] \\ [0] & [M_1] - C_d\, Re_1^2 [K_1] \end{bmatrix}$$

Then Eqn. (2.55) can be re-written as

$$[M]^{(e)} \{\ddot{q}\}^{(ne)} + [G]^{(e)} \{\dot{q}\}^{(ne)} + ([KD]^{(e)} - \Omega^2 [MD]) \{q\}^{(ne)} = \{FB\}^{(ne)} \quad \ldots\ (3.7)$$

Assuming a solution of the form

$$\{q\}^{(n)} = \{q_o\}^{(n)}\ e^{i\lambda' t} \quad \ldots\ (3.8)$$

and applying to assembled form of Eqn.(3.7) and noting the condition Eqn. (3.5), the eigen value problem becomes

$$[KD]\{q_o\}^{(n)} = \Omega^2 [MD] \{q_o\}^{(n)} \quad \ldots\ (3.9)$$

in which, the eigen values represent critical speeds in forward precession and Eqn. (3.9) is solved using NAG library subroutine F02AEF.

For critical speeds in backward precession, the critarion in XYS frame of reference is

$$\lambda = -\ \Omega \quad \ldots\ (3.10)$$

Then, from Eqn. (2.45), the criterion in I III frame becomes

$$\lambda' = -2\Omega \qquad \ldots\ldots (3.11)$$

Assuming solution of the form given by Eqn. (3.8) and applying to the assembled form of Eqn. (3.7), the eigen value problem to be solved becomes

$$[KD]\{q_0\} = \Omega^2 (4[M] + i2[G] + [MD])\{q_0\} \quad \ldots\ldots (3.12)$$

where the eigen values represent the critical speeds in backward precession. Now as one matrix is complex, the above eigen value problem is solved using the NAG library subroutine F02GJF.

The critical speeds of a dual shaft with shear deformation effect are also obtained using a similar procedure.

3.1.3 Isotropic shaft with damping :

The natural frequencies for this case are obtained solving Eqn. (2.67), for a range of spin speeds, using the method of solution giveb below.

The Eqn. (2.67), after assembling and applying boundary conditions becomes

$$[M]\{\ddot{q}\}^{(n)} + [C]\{\dot{q}\}^{(n)} + [K]\{q\}^{(n)} = 0$$

which can be re-written as [20]

$$\begin{bmatrix} [0] & [M] \\ [M] & [C] \end{bmatrix} \{\dot{P}\} + \begin{bmatrix} -[M] & [0] \\ [0] & [K] \end{bmatrix} \{P\} = 0 \quad \ldots\ldots (3.13)$$

where $\{P\} = \begin{Bmatrix} \{\dot{q}\} \\ \{q\} \end{Bmatrix}$

Assuming a solution of the form

$$\{P\} = \{P_o\} \; e^{\lambda t} \quad \ldots\ldots (3.14)$$

where $\lambda = \lambda_R + i\lambda_i$ is complex, Eqn. (3.13) becomes an eigen value problem of the form

$$\begin{bmatrix} [0] & [I] \\ -[K]^{-1}[M] & -[K]^{-1}[C] \end{bmatrix} \{P_o\} = \frac{1}{\lambda} \{P_o\} \ldots\ldots (3.15)$$

The above eigen value problem is solved using NAG library subroutine F02AFF. The eigen values appear as complex conjugate pairs, with positive or negative real parts. The positive real part indicates an instability.

3.2 CONVERGENCE STUDY :

To study the convergence, results (critical speeds) were obtained for a steel shaft of uniform circular section, using 4,6 and 8 elements, by solving Eqn. (3.4), for

hinged-hinged, fixed-fixed and cantilever boundary conditions. The value of material constant ($Mc = \frac{E}{K'G}$) for such a steel shaft is 2.9. The value of rotatory inertia co-efficient ($Re = \sqrt{\frac{I}{A^2}}$) used is 0.05, which represents a shaft having a length, five times its diameter.

The results are presented in Table.1.For hinged-hinged boundary conditions the results are compared with the closed form solution given by Dimentberg [4]. For other boundary conditions, comparison is done with the results obtained by Gocl [16] using transfer FEM with a single fourth order governing differential equation.

With an increase in number of elements used, the results converge from above and the error is larger in higher modes, as is to be expected by FEM. The critical speeds obtained using 8 elements were found to give accurate results for all the boundary conditions for the number of modes studied. Hence 8 elements were used for all the cases studied in this work.

Table 1 : Convergence Study of Critical Speeds

(Re = 0.05, Mc = 2.9)

Hinged-Hinged Shaft

Mode	No. of elements 4	6	8	Exact [4]
1	9.6387	9.6383	9.6383	9.6383
2	35.8967	35.8793	35.8774	35.8768
3	72.3132	72.1620	72.1429	72.1370
4	113.6066	112.3852	112.2958	112.2660
5	156.3399	153.5009	153.2122	153.1123

Fixed-Fixed Shaft

Mode	No. of elements 4	6	8	8 [16]
1	19.3408	19.3379	19.3377	21.660
2	47.0807	47.0430	47.0387	54.682
3	81.5682	81.3770	81.3501	94.827
4	120.4545	118.9859	118.8833	136.970
5	161.4977	158.0973	157.8044	-

Cantilever Shaft

Mode	No. of elements 4	6	8	8 [16]
1	3.4770	3.4770	3.4770	3.477
2	20.4524	20.4492	20.4490	20.441
3	52.0531	51.9979	51.9915	51.902
4	90.4899	90.2031	90.1609	89.801
5	132.9002	130.9754	130.8163	-

3.3 ISOTROPIC SHAFT WITHOUT DAMPING :

3.3.1 Effect of gyroscopic action and rotatory inertia :

Gyroscopic action term is the [G] matrix in Eqn. (2.29). Neglecting this term, the equations become as those of Timoshenko beam. Results (critical speeds) for forward precession for various shafts are compared with those of Timoshenko beams for Re values of 0.0125 and 0.05 in Table 2.

Results for hinged-hinged and cantilever shaft match well with the exact results of [4] and [16], but there is large difference for fixed-fixed shaft. This can be explained by noting that Goel's [16] results are based on single governing fourth order differential equation, whereas present results are based on two second order differential equations. In Goel's [16] approach one can satisfy only one geometrical boundary condition (GBC) Z = 0 exactly. Other geometrical boundary condition of slope and two natural boundary (NBC) conditions on shear and bending moment can be satisfied only in an approximate way whereas in the present approach all boundary conditions (geometrical and natural) can be satisfied exactly. In case of hinged-hinged shaft, Goel's approach satisfies two GBC exactly and two NBC approximately. And for fixed-fixed shaft it satisfies two GBC exactly and other two GBC approximately. It is seen that approximate application of two GBC in case of fixed-fixed shafts leads to a large error.

Table 2 : Study of gyroscopic and rotatory inertia effects on critical speeds :

(Mc = 2.9)

Hinged-hinged

Mode	Re = 0.0125				Re = 0.05			
	Timoshenko beam	Shaft			Timoshenko beam	Shaft		
		Goel	16	Present		Goel	16	Present
1	9.84	9.85		9.86	9.43	9.64		9.64
2	39.02	39.26		39.25	33.80	35.89		35.88
3	86.58	87.77		87.70	68.47	72.22		72.14
4	151.14	154.81		154.43	103.11	112.66		112.30
5	231.11	-		238.43	141.54	-		153.21

Fixed-fixed

Mode	Re = 0.0125				Re = 0.05			
	Timoshenko beam	Shaft			Timoshenko beam	Shaft		
		Goel	16	Present		Goel	16	Present
1	22.11	23.34		22.15	19.21	21.66		19.34
2	60.02	61.29		60.42	45.04	54.68		47.04
3	115.42	119.39		116.97	76.53	94.83		81.35
4.	186.47	195.84		190.53	110.85	136.97		118.88
5	271.53	-		279.92	146.96	-		157.80

Cantilever

Mode	Re = 0.0125				Re = 0.05			
	Timoshenko beam	Shaft			Timoshenko beam	Shaft		
		Goel	16	Present		Goel	16	Present
1	3.51	3.51		3.51	3.94	3.48		3.48
2	21.82	21.93		21.93	19.23	20.44		20.45
3	60.32	61.03		61.01	47.14	51.90		51.99
4	116.10	118.62		118.46	80.15	89.80		90.16
5	187.83	-		193.57	115.91	-		130.82

It is seen that, the effect of gyroscopic action is to increase the natural frequency of the system and the effect is significant in higher modes. This is because, the moments arising due to the gyroscopic action, try to straighten the shaft, and thus account for an increase in effective stiffness, which increases the natural frequencies of the system. The gyroscopic moments increase with increase in curvature. As the curvature is larger in higher modes, the effect is of appreciable magnitude in higher modes. The effect is seen to increase with an increase in Re. A larger Re implies a thicker shaft (i.e. a smaller l/d ratio, where d is the diameter of shaft), which also leads to larger gyroscopic moments, and hence an increased effect.

It is also seen that critical speeds decrease with increase in Re value, and this effect is significant in higher modes, as expected.

5.5.2 Effect of shear deformation :

Critical speeds in forward precession are obtained by solving Eqns. (2.31), and are given Table 3 for various shafts, for two values of Re. Results with shear are also given in this table.

It is clear from Table 3, that neglecting shear deformation effect leads to an over-estimation of critical speeds and the effect is of appreciable magnitude for thicker shafts (i.e. higher Re), which is as expected. For Re = 0.05

Table 3 : Study of shear deformation effect on critical speeds.

(Mc = 2.9)

Hinged-hinged

Mode	Re = 0.0125		Re = 0.05	
	Without shear	With shear	Without shear	With shear
1	9.88	9.86	9.99	9.64
2	39.61	39.25	41.60	33.88
3	89.57	87.70	100.84	72.14
4	160.53	154.43	203.81	112.30
5	253.98	238.44	402.69	153.21
6	518.80	338.57	1092.45	193.89
7	739.01	453,71	-	234.20
8	933.83	589.84	-	275.21

Fixed-fixed

Mode	Re = 0.0125		Re = 0.05	
	Without shear	With shear	Without shear	With shear
1	22.40	22.15	22.73	19.38
2	61.94	60.42	65.60	47.04
3	122.14	116.97	139.66	81.35
4	203.86	190.53	266.20	118.88
5	308.94	279.92	521.53	157.80
6	439.68	383.80	1926.30	197.16
7	592.05	500.15	-	236.59
8	847.90	539.98	-	277.08

Table 3....(contd.) Cantilever

Mode	Re = 0.0125		Re = 0.05	
	Without shear	With shear	Without shear	With shear
1	3.52	3.51	3.54	3.48
2	22.09	21.93	22.99	20.45
3	62.11	61.01	68.72	51.99
4	122.55	118.46	150.87	90.16
5	204.72	193.57	303.32	130.82
6	310.38	285.20	679.33	171.84
7	441.62	392.04	-	212.56
8	593.75	511.67	-	252.90

only six critical speeds are obtained in forward precession for all the three shafts. This confirms the work of Dimentberg [4] , who showed by close-form solution that the number of critical speeds (n) in forward precession is limited by(for hinged-hinged supports).

$$n \leq \frac{1}{\pi Re} \quad \ldots\ldots (3.16)$$

Observing the results for fixed-fixed and cantilever support conditions, it seems that above relation holds good for these shafts also.

3.3.3 Multi-span shafts:

Three shafts with two, three and four spans used by Goel [16] are studied and are shown in Table 4. All supports are hinged. Number of elements used in each span are shown in brackets. Critical speeds are presented in Table 4. Also presented are the results of rotor given by Goel using transfer FEM.

With increase in number of supports, the stiffness of the system increases significantly. Hence, a significant increase in critical speeds is to be expected, and it is clear from Table 4.

Except the results for first mode for three and four span shafts, the present results are comparable with those of Goel [16]. These two results for the first mode are clearly in error as they violate the fact that increase in number of

Table 4 : Critical speeds for multi-span rotors

(Re = 0.05 , Mc = 2.0)

Note : 1) The numbers on top are the ratio of span length/ total length

2) The numbers between two supports are the number of elements considered for that span,

Two-span rotor:

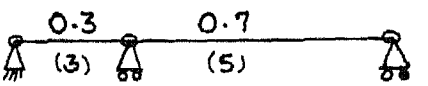

Mode	Rotor	
	Present	Goel [16]
1	23.98	24.95
2	69.60	70.62
3	93.87	104.22
4	128.92	138.36

Three-span rotor :

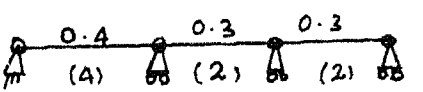

Mode	Rotor	
	Present	Goel [16]
1	60.10	23.88
2	89.88	86.40
3	113.42	111.91
4	160.22	142.26

Four-span rotor :

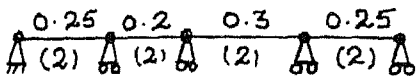

Mode	Rotor	
	Present	Goel
1	100.26	31.69
2	121.12	112.63
3	128.78	133.25
4	180.64	162.73

supports increases the stiffness significantly. Moreover these types of inaccuracies are quite common in transfer FEM. Otherwise results differ, as Goel [16] used a fourth order differential equation and present work uses two second order differential equations.

3.4 EFFECT OF SHAFT MASS AND DISK FLEXIBILITY :

As said earlier, most of the work in rotor dynamics neglects the mass of the shaft and the flexibility of the disk. Effect of these assumptions is studied in this section.

To study the effect of shaft mass, a steel shaft of 1000 mm length and 40 mm diameter with hinged-hinged supports is chosen. This shaft has a rigid disk of 30 mm thickness and 90 mm diameter placed at a distance of 250 mm from the left end. For shaft, rotatory and gyroscopic effects are taken into consideration, i.e. governing equations are (2.31). Shaft is divided into eight equal length elements. Disk is taken to be rigid, but has rotatory and gyroscopic effects. Thus for the disk at node 3, one has [4]

$$\begin{bmatrix} m_d & 0 \\ 0 & I_d \end{bmatrix} \begin{Bmatrix} \ddot{Z}_3 \\ \ddot{\gamma}_3 \end{Bmatrix} - i \begin{bmatrix} 0 & 0 \\ 0 & I_p \Omega_o \end{bmatrix} \begin{Bmatrix} \dot{Z}_3 \\ \dot{\gamma}_3 \end{Bmatrix} = \begin{Bmatrix} 0 \\ 0 \end{Bmatrix} \quad \ldots\ldots (3.17)$$

where m_d is the mass of disk, I_d and I_p are the diametral and polar mass moment of inertia of disk, and Ω_o is the spin speed of shaft. Equation (2.31) and Eqn. (3.17) were assembled together and solved for critical speeds for a range of shaft mass. Range of shaft mass is obtained by successively decreasing the density of shaft and maintaining all other parameters (length, diameter and E) constant so as not to alter the stiffness of shaft. Critical speeds for first five modes as a function of ratio of shaft mass to disk mass are given in Table 5.

The critical speeds for massless shaft are obtained by reducing the order of assembled stiffness matrix to that of mass matrix of disk i.e. 2x2, using static condensation [27]. For static condensation, see Appendix III. For forward precession, only one critical speed exists and is shown in Table 5. This is same as the close form solution given by Tse [22].

It is seen for this shaft and disk, in the first mode there is an error of 158 % for a shaft to disk mass ratio of 6.584 and 30 % for a shaft to disk mass ratio of 0.844. Moreover massless shaft assumption gives only one mode in forward precession. Thus one should not neglect the shaft mass, as error can be considerable even in first mode when shaft and disk mass are comparable.

Table 5 : Effect of shaft mass on critical speeds

(8- elements)

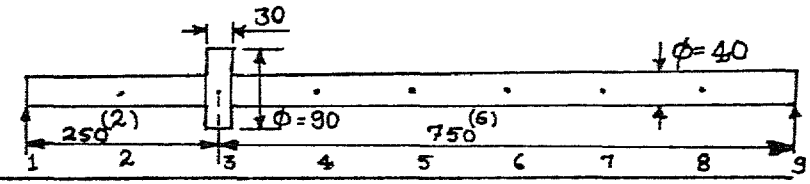

Mode	Shaft density in kg/m3					
	7806.0	4000.0	1000.0	100.0	10.0	0.0
	Ratio of shaft mass to disk mass					
	6.584	3.374	0.844	0.084	0.008	0.0 Present and [22]
1	473.1	621.4	940.2	1183.9	1218.3	1222.2
2	1806.9	2346.7	3948.9	11208.5	37761.7	-
3	4392.1	6020.3	11771.4	39038.6	127728.2	-
4	8326.1	11758.3	24720.8	84446.9	269893.9	-
5	12357.2	16899.8	33344.4	112280.9	360722.6	-

To study the effect of flexibility of disks, two shafts, one with single disk and other with two disks, shown in Table 6 are studied. Disk is treated as a standard shaft element. For the first shaft there are eight elements when disk is taken as rigid and nine elements when disk is flexible. For second shaft with two disks, there are eight elements when disks are taken as rigid and ten elements when disks are taken as flexible.

The results are presented in Table 6. The critical speeds obtained assuming the disks to be flexible are higher than those obtained considering the disks to be rigid, as expected. In the first mode the difference in results is 3.2 % for shaft with one disk and 8.1 % for shaft with two disks.

3.5 DUAL SHAFT :

A steel dual shaft with following parameters has been chosen for this study.

$$C = \frac{I_1}{I_2} = 1.5 \ , \ Re_1 = 0.05, \ C_d \ (= \frac{k^2}{k_1^2}) = 1.0$$

Critical speeds for this dual shaft with no shear deformation are obtained from Eqns. (2.55), and with shear deformation from Eqns. (2.53). For without shear case, results for forward and backward precession are obtained and are given in Table 7. With shear case results, for forward precession are obtained and are also given in the same table.

Table 6 : Effect of flexibility of disks on critical speeds.

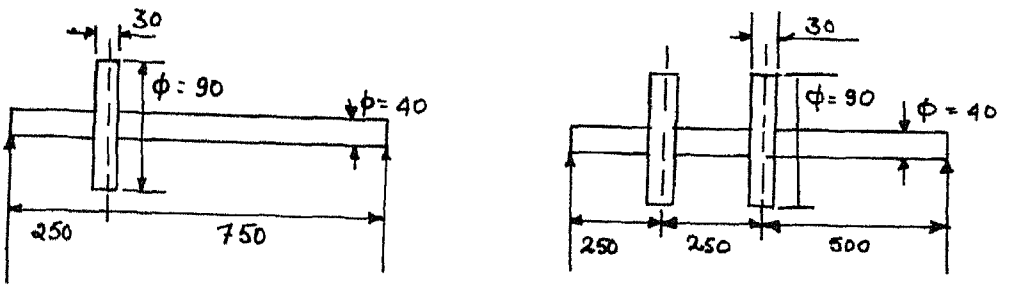

Mode	One disk		Two disks	
	Rigid	Flexible	Rigid	Flexible
1	473.1	488.6	420.9	457.8
2	1806.9	1910.4	1800.5	1911.1
3	4392.1	4498.3	3883.8	4231.7
4	8326.1	8508.6	8304.6	8470.8
5	12357.2	12824.8	11506.6	12392.5

For forward precession, close form solutions for hinged-hinged shafts are available [4] and are given in Table 7. Present FEM results match well with these. It is seen that dual stiffness has doubled the number of critical speeds when compared to the corresponding isotropic shaft. Further, as can be seen from the eigen value problem Eqn. (3.9), for forward mode of precession, the vibration in the two principal planes (IS and IIS) become uncoupled. Since the elastic properties are different in the two principal planes, there will be a critical speed critical-speed corresponding to the elastic property in each plane, leading to doubling of critical speeds in comparison to isotropic shaft.

The critical speeds in backward mode of precession are also presented in Table 7. Also presented are, the critical speeds from [4], for hinged-hinged support conditions. By observing the eigen value problem, Eqn. (3.12), it is seen that the vibrations in two planes are coupled by the [G] matrix. Multiple critical speeds are seen to exist in backward mode, in contrast to forward mode.

3.6 ISOTROPIC SHAFT WITH DIFFERENT SUPPORT CONDITIONS IN TWO PLANES :

In this section, the results are obtained for an isotropic shaft with different support conditions in two planes. Solution is obtained from equations of dual shaft, Eqn. (2.53),

Table 7 : Critical speeds of a dual shaft.

(8-elements)

Without shear deformation (forward pression)

($C = \frac{I_1}{I_2} = 1.5$, $Re_1 = 0.05$, $C_d = 1.0$)

Mode	Hinged-hinged		Fixed-fixed	Cantilever
	Present	Exact 4		
1	8.16	8.16	18.57	2.89
2	9.99	9.99	22.73	3.54
3	33.96	33.95	53.56	18.77
4	41.60	41.59	65.60	22.99
5	82.34	82.30	114.03	56.11
6	100.84	100.71	139.66	68.72
7	166.41	165.74	217.36	123.18
8	203.81	202.99	266.20	150.87

With shear deformation (forward precession)

(Mc= 2.9, $\frac{I_1}{I_2} = 1.5$, $Re_1 = 0.05$, $C_d = 1.0$)

Mode	Hinged-hinged		Fixed-fixed	Cantilever
	Present	Exact 4		
1	7.96	7.88	16.57	2.86
2	9.64	9.54	19.34	3.48
3	30.61	29.44	41.87	17.31
4	35.88	34.55	47.04	20.45
5	64.07	59.82	74.61	40.70
6	72.14	67.74	81.35	52.00
7	103.22	94.33	111.50	82.18
8	112.30	103.79	118.88	90.20

Table 7. (...Contd.., Without shear deformation (Backward precession)

$(C\ (= \frac{T_1}{T_2}) = 1.5,\ Re_1 = 0.05,\ C_d = 1.0)$

Mode	Hinged-hinged		Fixed- Fixed	Cantilever
	Present	Exact [4]		
1	2.92	2.92	6.62	3.16
2	8.72	8.72	17.99	6.48
3	11.55	11.54	19.60	17.75
4	25.48	25.45	34.58	18.11
5	31.77	31.76	48.69	33.97
6	44.20	44.02	55.77	45.09
7	63.16	63.07	80.98	54.56
8	67.14	66.54	84.23	77.54
9	93.88	92.22	109.73	79.04
10	98.44	98.06	122.16	106.63

using $C=C_d = 1$. This shaft has hinged supports in IL plane and fixed supports in IIL plane. Using these boundary conditions the forward critical speeds are obtained and are given in Table 8. Also given are the critical speeds, for similar fixing conditions in two planes i.e. similar fixing conditions of hinged and fixed supports.

It is noted that critical speeds of different support conditions, HF-HF, can be obtained by combining the critical speeds of shafts of isotropic support conditions of HH-HH and FF-FF. Thus, there are two critical speeds in comparison to a shaft having similar fixing conditions in the two planes of deflections. Critical speeds due to vibrations in each plane correspond to the support conditions in the respective planes. Hence it may be said that an isotropic shaft having dissimilar support conditions, behaves in a manner similar to a dual shaft having similar support conditions, with regards to critical speeds.

Table 8 : Forward critical speeds with dissimilar support conditions.

(Mc = 2.9, Re= 0.05, 8 elements)

H: Hinged support ; F : Fixed supports

Mode	HH-HH	HF-HF	FF-FF
1	9.64	9.64	19.34
2	35.88	19.34	47.04
3	72.14	35.88	81.35
4	112.30	47.04	118.88
5	153.21	72.14	157.80
6	193.89	81.35	197.16
7	234.20	112.30	236.59
8	275.21	118.88	277.08

3.7 ISOTROPIC SHAFT WITH DAMPING :

To study the effect of internal viscous and hysteretic damping, the Eqns. (2.67) are solved. A steel shaft with $Re = 0.02$ (i.e. $\frac{l}{d} = 12.5$) studied by [9] , with hinged-hinged support conditions is chosen. The bearings are assumed to have uncoupled stiffness and damping charecteristics i.e. $K_{xy} = K_{yx} = 0$ and $C_{xy} = C_{yx} = 0$. The complex frequencies are obtained in the form of

$$\lambda = \lambda_R + \lambda_I \qquad \ldots\ (3.18)$$

The nondimensional frequencies are plotted in Figs. (3.1) to (3.5), for a speed range of 0 to 17 (i.e. 0 to 12000rpm), and for various combinations of, bearing flexibility and bearing damping charecteristics.

The curves labelled "F" and "B" represent forward and backward precessional modes respectively. In all the cases studied, the results are compared with the results of [9] . The observations made in each case are listed below.

Case 1 : Viscous damping, isotropic undamped bearings.

Bearings are undamped and have isotropic support conditions of

$$K_{xx} = K_{yy} = 33.14 \ (17.5 \text{ MN/m})$$

Considering the internal damping to be viscous, with $\eta_{VN} = 0.01621$ (0.0002s), natural frequencies obtained are given in Fig. (3.1) as function of speed Ω . The

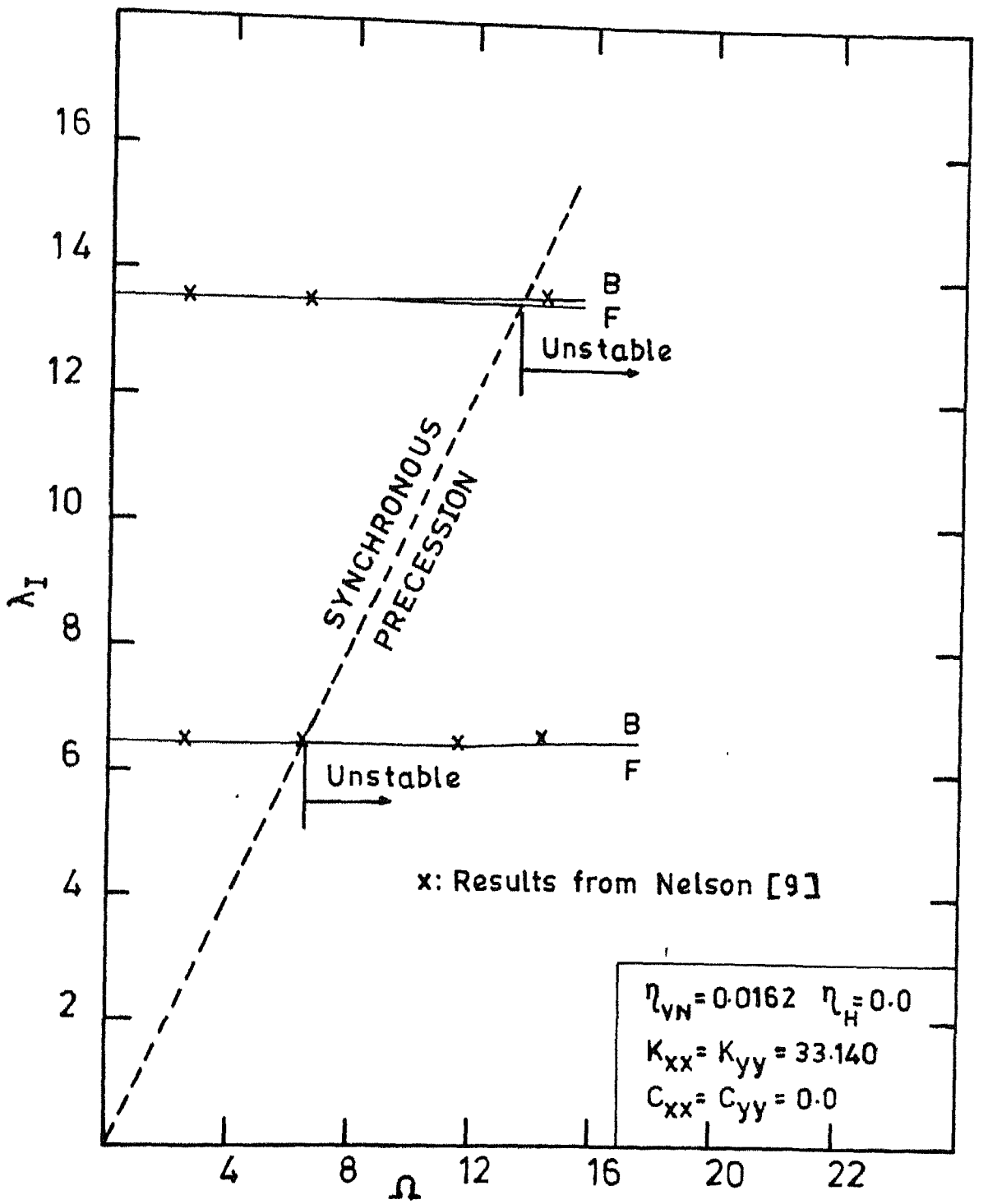

Fig. 3.1 Natural frequency λ_I vs. spin speed Ω for case 1.

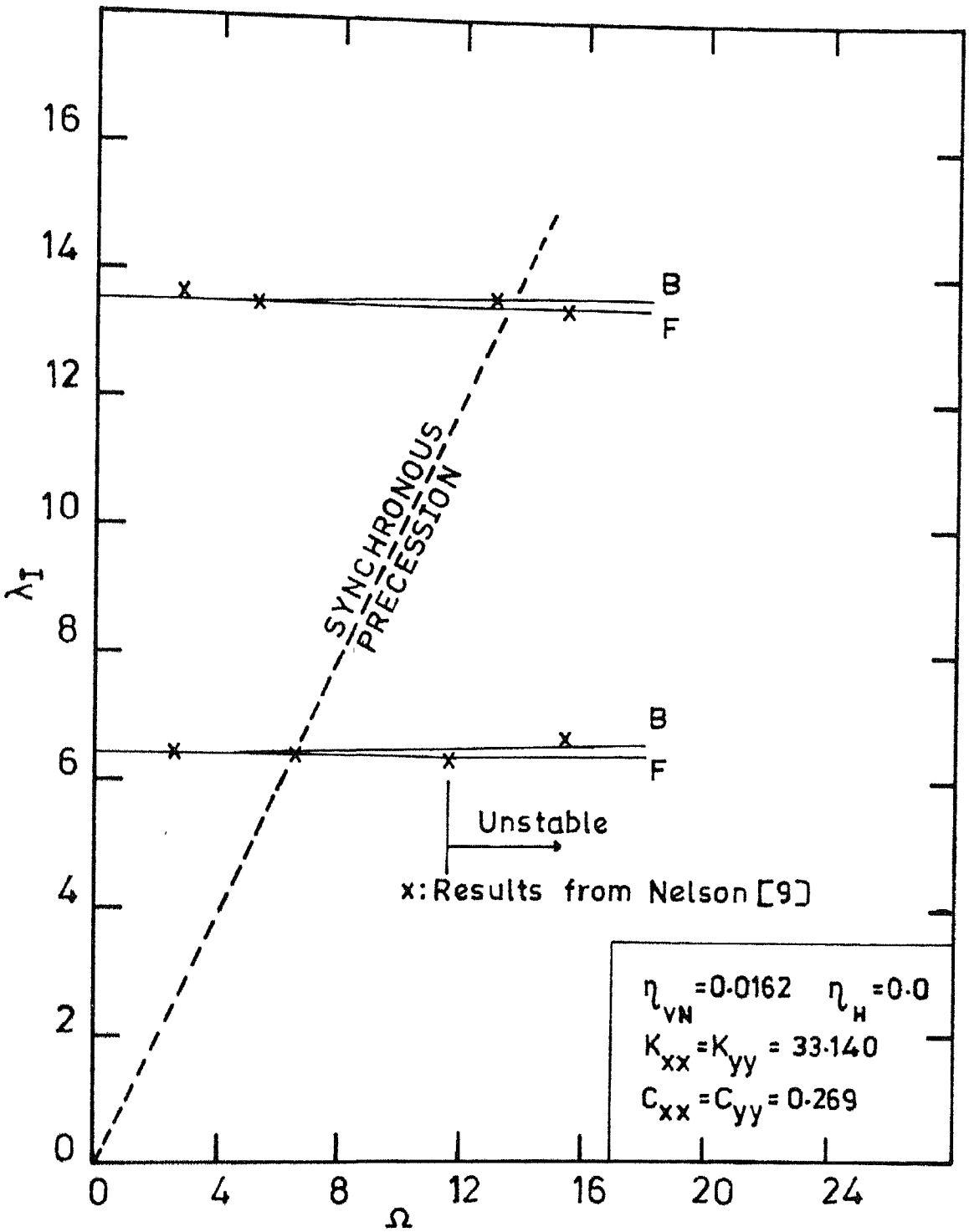

Fig.3.2 Natural frequency λ_I vs. spin speed Ω for case 2

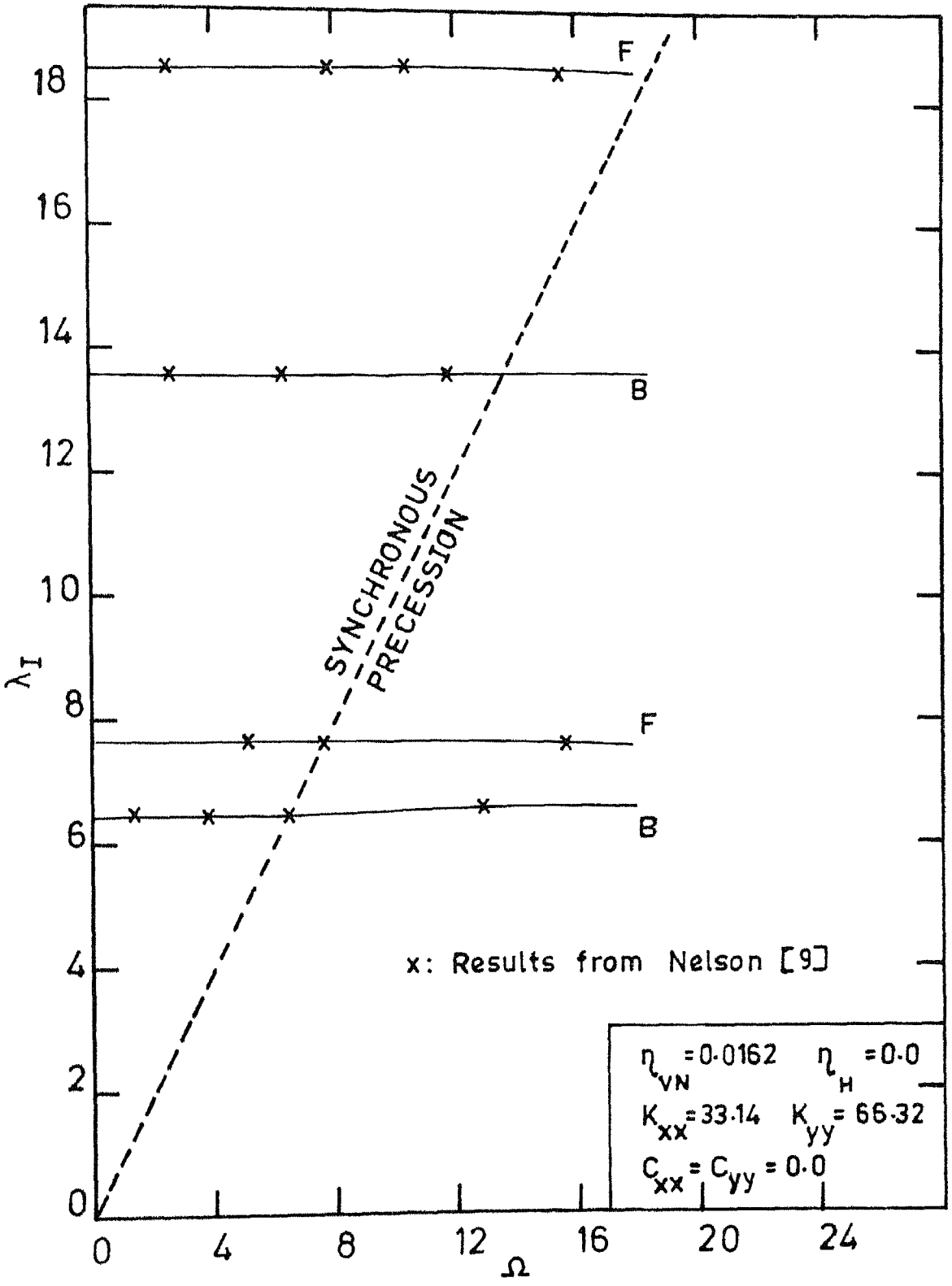

Fig. 3.3 Natural frequency λ_I vs. spih speed Ω for case 3

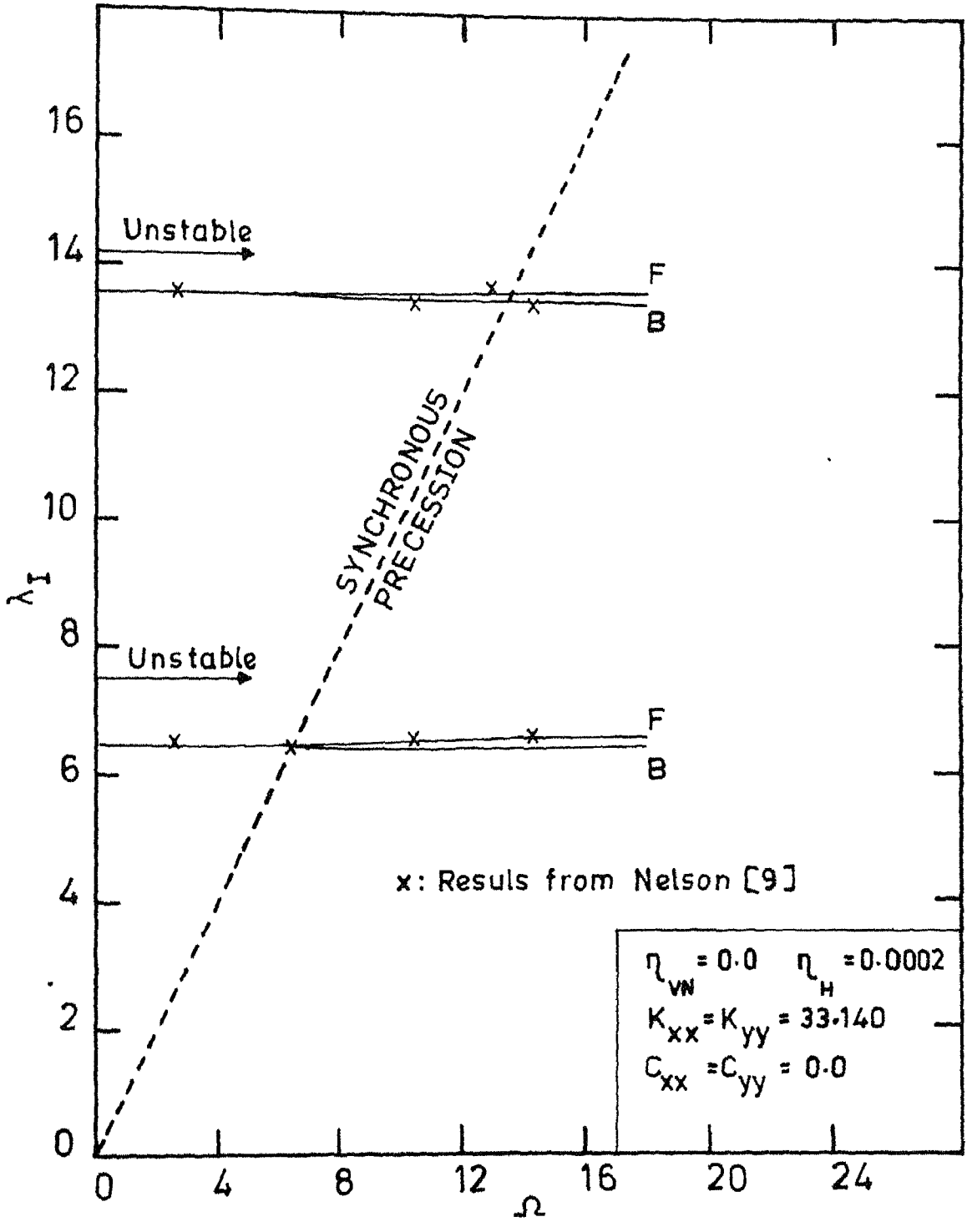

Fig. 3.4 Natural frequency λ_I vs spin speed Ω for case 4

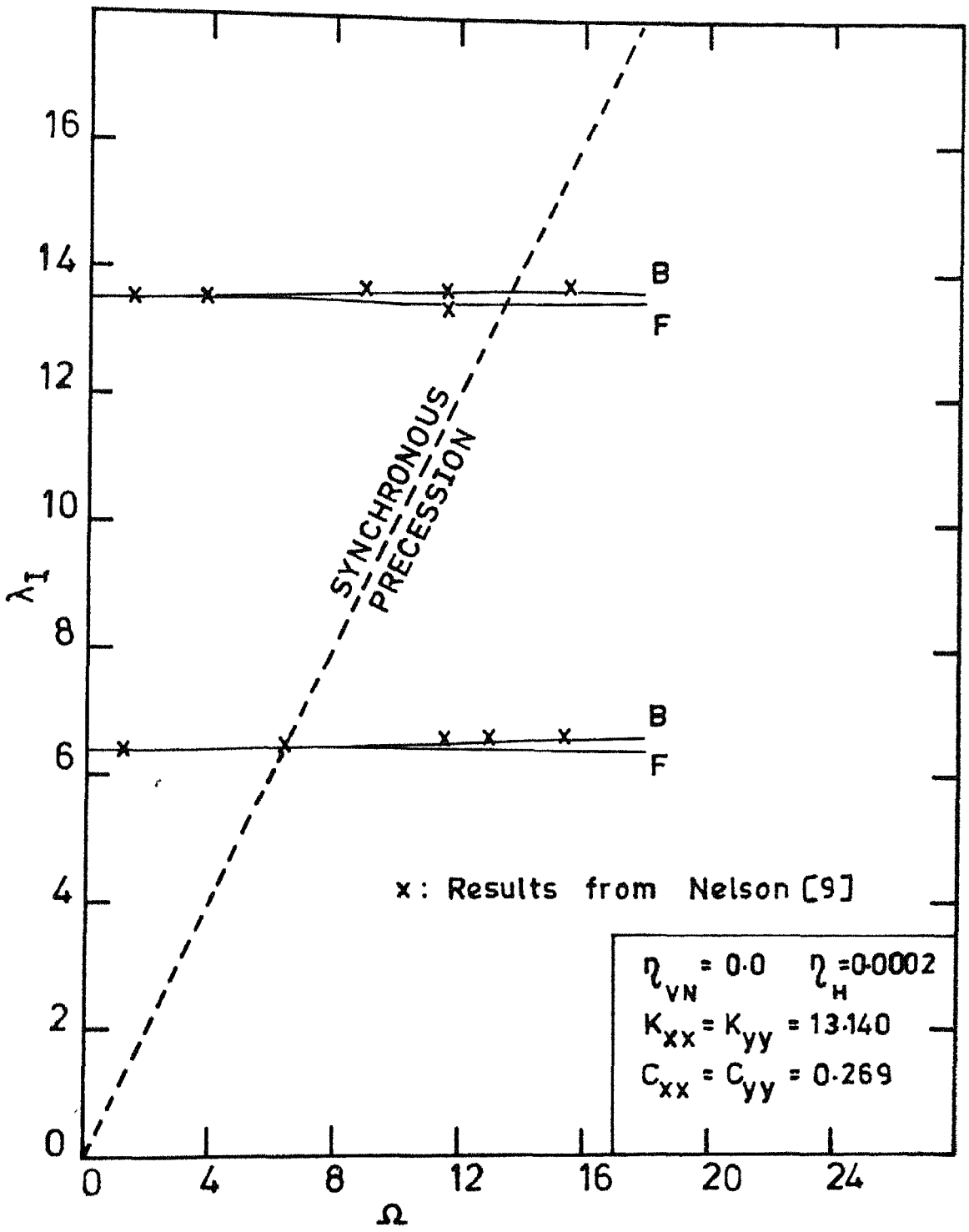

Fig. 3.5 Natural frequency λ_I vs spin speed Ω for case 5

first critical speed occurs at 6.44 (4980 rpm) and second critical speed occurs at 13.55 (10500 rpm) in forward mode of precision. These values are in good agreement with those given by [9] , which are 6.40 (4950 rpm) and 13.55, The first mode was found to become unstable at the first forward critical speed and the second mode at second forward critical speed. These modes stay unstable upto the studied speed range (15.5).

Case 2 : Viscous damping, isotropic damped bearings.

The system studied in case 1 is analysed incorporating isotropic bearing dampings with $C_{xx} = C_{yy} = 0.269$ .. (i.e. $1.75 \times 10^3 \frac{N.s}{m}$) where C_{xx}, C_{yy} represent the bearing damping coefficients in non-dimensional form in X and Y directions respectively. The results are plotted in Fig.(3.2). It is seen that, the first mode in now stable upto speed of 11.6(9000 rpm) and the second mode is stable for the entire spin speed range studied (15.5). The results match very well with [9].

Case 3 : Viscous damping, anisotropic undamped bearings.

Shaft has viscous damping $\eta_{VN} = 0.0162$. Bearings are undamped and support conditions are anisotropic i.e.

$K_{xx} = 33.140$, $K_{yy} = 66.318$,

The results are shown in Fig. (3.3). It is seen that the system becomes stable for the entire spin speed range studied. Forward and backward precessional speeds are wide apart now. Results match very well with [9] .

Case 4 : Hysteretic damping, isotropic undamped bearing .

The effect of hysteretic damping is studied in this case. Bearings are undamped and have isotropic support conditions

$$K_{xx} = K_{yy} = 33.14$$

The value of loss factor η_H used is 0.0002. The results are plotted in Fig. (3.4). It is seen that both forward precessional modes become unstable and both backward modes are stable for the entire spin speed range studied. As before forward and backward precessional speeds are quite close to each other in the modes studied. Results match very well with [9] .

Case 5 : Hysteretic damping, isotropic damped bearings .

Isotropic damped bearings with following properties are used.

$$K_{xx} = K_{yy} = 33.14$$

$$C_{xx} = C_{yy} = 0.269$$

Value of loss factor η_{II} used is 0.0002.

The results are shown in Fig. (3.5). It is seen that both the modes are stable for the entire speed range studied. The results match well with [9]. Forward and backward precessional speeds are quite close to each other.

Internal viscous damping is seen to have destabilising effect beyond the first critical speed in forward mode. The stability of the system is improved by providing damped bearings. Stability is improved further by the provision of bearings having anisotropic stiffness properties. Internal hysteretic damping destabilises all the forward modes over the entire speed range. The provision of damped bearings is again seen to improve the stability of the system.

3.7.1 Effect of bearing stiffness on stability :

For the shaft studied in section (3.7), case 1, with the isotropic bearings, the instability was found to occure at the first critical speed. This case was further extended to analyse the effect of bearing stiffness on the instability threshold. Instability threshold speeds are obtained for a range of values of isotropic bearing stiffness. The results are given in Fig. (3.6). It is seen that, the instability threshold increases with increase in bearing stiffness significantly in the begining.

3.7.2 Effect of bearing damping on stability :

The shaft studied in Section (3.7.1), is analysed to study the effect of variation in bearing damping properties at a few chosen bearing stiffness values, on the instability

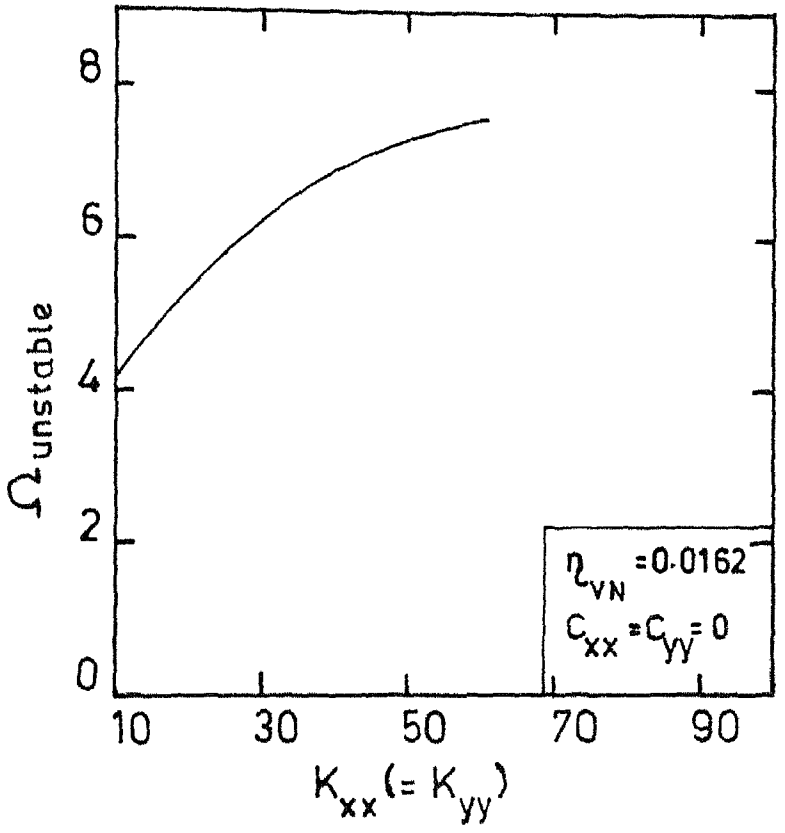

Fig. 3.6 Variation in instability threshold with bearing stiffness

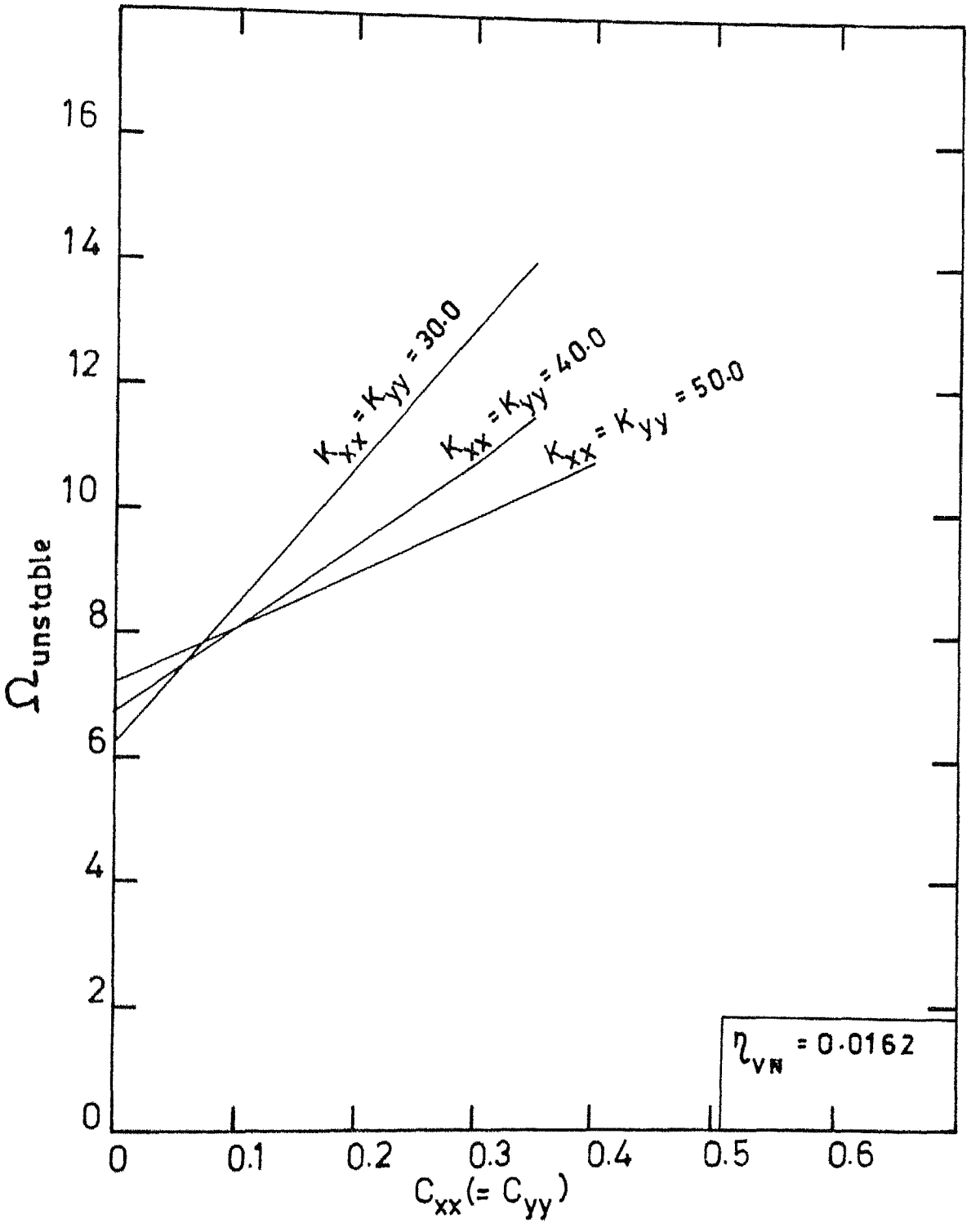

Fig. 3.7 Bearing damping vs. instability threshold

threshold speed, for the first mode. The results obtained are plotted in Fig. (3.7). It is seen that with an increase in bearing damping coefficient the instability threshold increases linearly. The instability threshold is seen to be decreasing with an increase in stiffness of bearings, when bearing damping is present. Thus a lower value of bearing stiffness, 30.0, and higher value of bearing damping, 0.35 ($2.28 \times 10^3 \frac{N-S}{m}$), are seen to give the highest stable speed range in the present case. But as can be seen from the Fig. (3.7) for a lower value of bearing damping coefficient, a bearing with higher stiffness gives better stability.

CHAPTER- IV

CONCLUSIONS

The following conclusions emerge out of the present work.

1. FEM is easily applicable to more familiar differential equations of rotor dynamics. It is simple and yields reliable results. Satisfaction of boundary conditions of intermediate supports (multi-span rotors) is straight forward.

2. When shear deformation effect is considered, results from two simultaneous second order partial differential equations using cubic polynomial approximation are very accurate (there is no ill conditioning). Geometrical and natural boundary conditions are satisfied exactly. Results obtained are accurate with fewer elements.

3. Neglecting shaft mass can lead to large errors. The mass of the shaft is taken care of in a routine way in FEM.

4. For undamped isotropic bearings, the instability threshold increases with increase in bearing stiffness significantly in the begining.

5. For lower value of bearing damping higher stiffness increases the stability, and this effect is reversed for higher values of bearing damping.

APPENDIX - I

DERIVATION OF KINETIC ENERGY

The shaft cross section has a rotation θ_x about X-axis, θ_y about Y-axis, θ_z about S-axis, translation x along X-axis and y along Y-axis, as mentioned in section (2.1). The kinetic energy due to rotation is obtained as follows

Consider a frame of reference abc attached to shaft cross section such that, c axis is normal to the cross section; a,b axes are in the plane of cross section and mutually perpendicular to each other and to c axis. Then the rotations of cross section relative to XYS frame are also the rotations of frame abc relative to XYS. Initially, the axes of abc frame are considered to be coincident with XYS frame. The final position of abc frame relative to XYS is determined by the following sequence of rotations.

1) A rotation by θ_x about X-axis gives $a_2b_2c_2$

2) A rotation by θ_y about b_2-axis gives $a_1b_1c_1$

3) A rotation by θ_z about c_1-axis gives abc

Referring to Fig. (A-1a) the position of $a_2b_2c_2$ frame after the rotation θ_x relative to XYS frame is

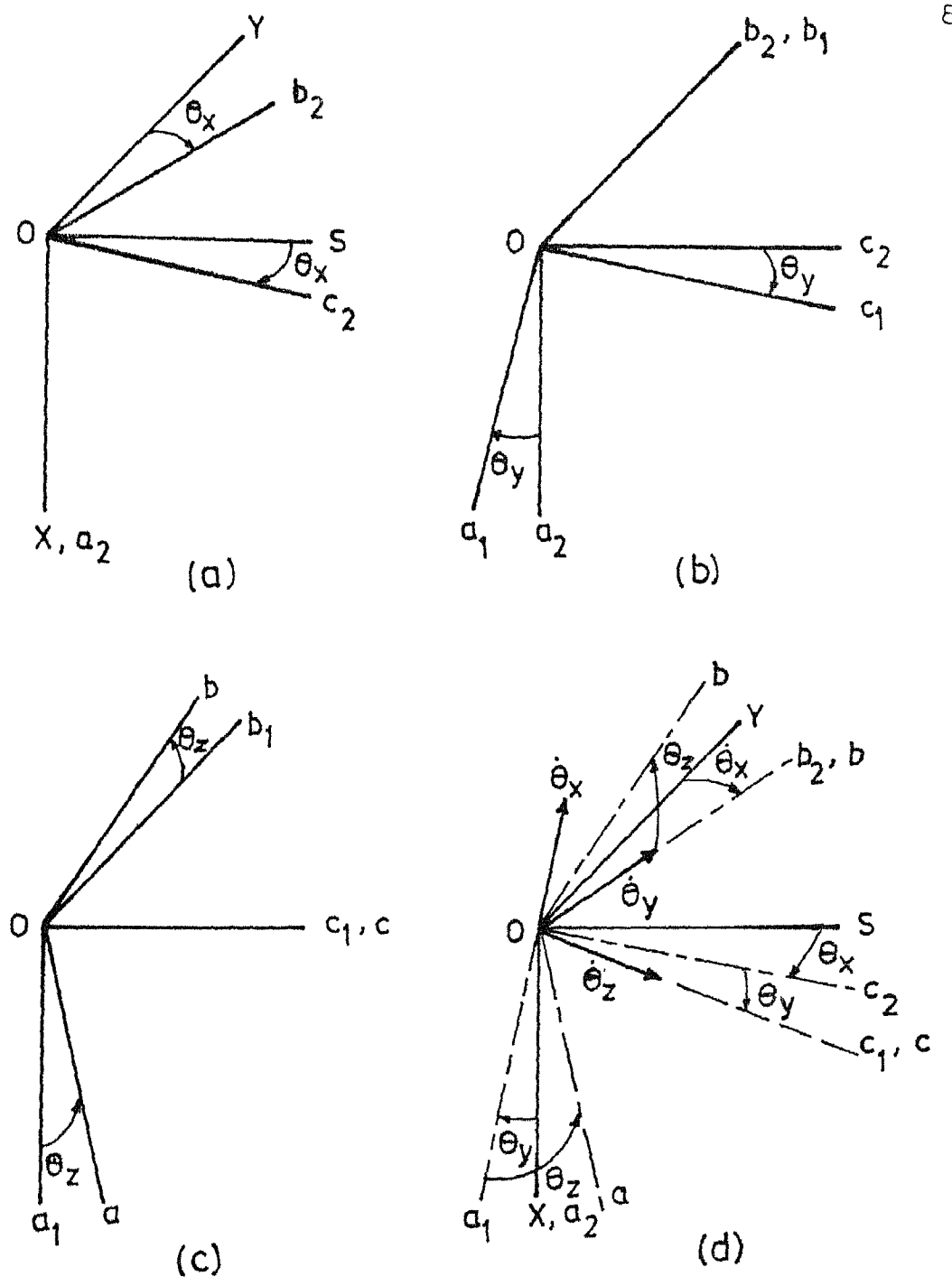

Fig. A-1 (a) Rotation by θ_x about X axis
(b) Rotation by θ_y about b_2 axis
(c) Rotation by θ_z about c_1 axis
(d) Final position of abc frame

$$\begin{Bmatrix} a_2 \\ b_2 \\ c_2 \end{Bmatrix} = \begin{bmatrix} 1 & 0 & 0 \\ 0 & \cos\theta_x & \sin\theta_x \\ 0 & -\sin\theta_x & \cos\theta_x \end{bmatrix} \begin{Bmatrix} X \\ Y \\ S \end{Bmatrix} \qquad (A\text{-}1.1)$$

Similarly the position of frame $a_1b_1c_1$ relative to $a_2b_2c_2$, after the rotation θ_y is, Fig. (A-1b),

$$\begin{Bmatrix} a_1 \\ b_1 \\ c_1 \end{Bmatrix} = \begin{bmatrix} \cos\theta_y & 0 & -\sin\theta_y \\ 0 & 1 & 0 \\ \sin\theta_y & 0 & \cos\theta_y \end{bmatrix} \begin{Bmatrix} a_2 \\ b_2 \\ c_2 \end{Bmatrix} \qquad (A\text{-}1.2)$$

Finally, the position of frame abc relative to frame $a_1b_1c_1$, after the rotation θ_z is, Fig. (A-1c)

$$\begin{Bmatrix} a \\ b \\ c \end{Bmatrix} = \begin{bmatrix} \cos\theta_z & \sin\theta_z & 0 \\ -\sin\theta_z & \cos\theta_z & 0 \\ 0 & 0 & 1 \end{bmatrix} \begin{Bmatrix} a_1 \\ b_1 \\ c_1 \end{Bmatrix} \qquad (A\text{-}1.3)$$

The final position of abc after the above rotations is shown in Fig. (A-1d). The frame abc has the angular velocities $\dot{\theta}_x$ along $-a_2$, see Fig. (A-2), $\dot{\theta}_y$ along b_1 and $\dot{\theta}_z$ along c. The components of $\dot{\theta}_x$ along the directions a,b and c can be obtained by the following transformation using Eqns. (A-1.2) and (A-1.3)

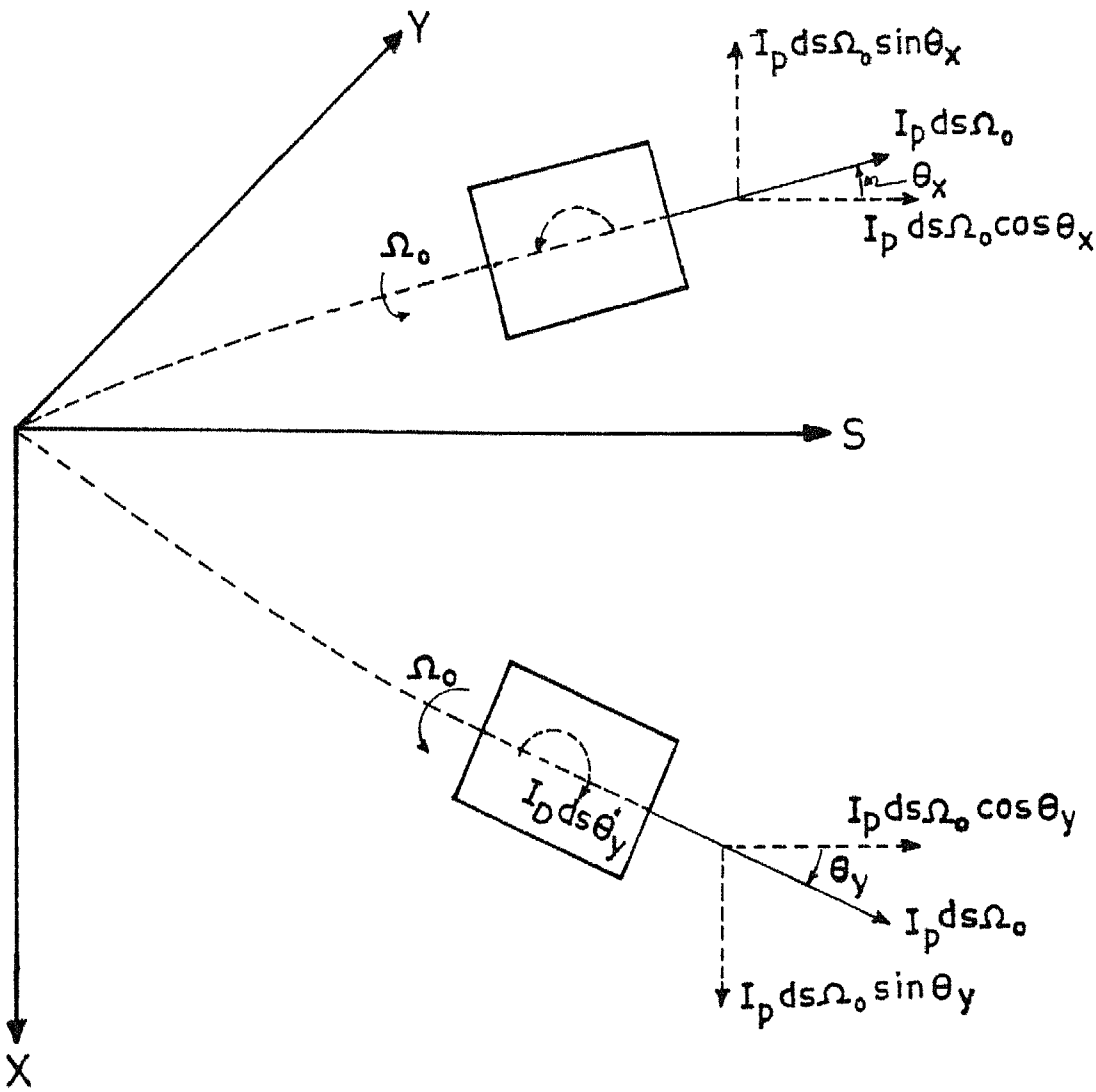

Fig. A-2 The angular momentums

$$\begin{Bmatrix} \dot{\theta}_{x,a} \\ \dot{\theta}_{x,b} \\ \dot{\theta}_{x,c} \end{Bmatrix} = \begin{bmatrix} \cos\theta_z & \sin\theta_z & 0 \\ -\sin\theta_z & \cos\theta_z & 0 \\ 0 & 0 & 1 \end{bmatrix} \begin{bmatrix} \cos\theta_y & 0 & -\sin\theta_y \\ 0 & 1 & 0 \\ \sin\theta_y & 0 & \cos\theta_y \end{bmatrix} \begin{Bmatrix} -\dot{\theta}_x \\ 0 \\ 0 \end{Bmatrix}$$

$$= \begin{Bmatrix} -\theta_x \cos\theta_y \cos\theta_z \\ \theta_x \cos\theta_y \sin\theta_z \\ -\theta_x \sin\theta_y \end{Bmatrix} \qquad (A\text{-}1.4)$$

Similarly the components of $\dot{\theta}_y$ along the directions a,b and c can be obtained using Eqn. (A-1.3) as

$$\begin{Bmatrix} \dot{\theta}_{y,a} \\ \dot{\theta}_{y,b} \\ \dot{\theta}_{y,c} \end{Bmatrix} = \begin{bmatrix} \cos\theta_z & \sin\theta_z & 0 \\ -\sin\theta_z & \cos\theta_z & 0 \\ 0 & 0 & 1 \end{bmatrix} \begin{Bmatrix} 0 \\ \dot{\theta}_y \\ 0 \end{Bmatrix}$$

$$= \begin{Bmatrix} \theta_y \sin\theta_z \\ \theta_y \cos\theta_z \\ 0 \end{Bmatrix} \qquad (A\text{-}1.5)$$

The angular velocity vector $\dot{\theta}_z$ is along c direction, thus no transformation is needed. Hence the angular velocities along a,b and c directions, due to the rotations θ_x, θ_y and θ_z are obtained using Eqns. (A-1.4) and (A-1.5) as

$$\begin{aligned}
\Omega_a &= \dot{\theta}_{x,a} + \dot{\theta}_{y,a} + \dot{\theta}_{z,a} = -\dot{\theta}_x \cos\theta_y \cos\theta_z + \dot{\theta}_y \sin\theta_z \\
\Omega_b &= \dot{\theta}_{x,b} + \dot{\theta}_{y,b} + \dot{\theta}_{z,b} = \dot{\theta}_x \cos\theta_y \sin\theta_z + \dot{\theta}_y \cos\theta_z \\
\Omega_c &= \dot{\theta}_{x,c} + \dot{\theta}_{y,c} + \dot{\theta}_{z,c} = -\dot{\theta}_x \sin\theta_y + \dot{\theta}_z
\end{aligned} \qquad (A\text{-}1.6)$$

As the directions a,b and c are also the principal directions, the kinetic energy due to translation and rotation becomes

$$T_e = \frac{1}{2} \int_0^l [\, m(\dot{x}^2+\dot{y}^2) + I_D(\Omega_a^2 + \Omega_b^2) + I_p \Omega_c^2 \,]\, ds \qquad (A\text{-}1.7)$$

Substituting Eqn. (A-1.6), the expression for kinetic energy becomes.

$$\begin{aligned}
T_e = \frac{1}{2} \int_0^l [\, & m(\dot{x}^2+\dot{y}^2) + I_D(\dot{\theta}_x^2 \cos^2\theta_y + \dot{\theta}_y^2) \\
& + I_p(\dot{\theta}_x^2 \sin^2\theta_y + \dot{\theta}_z^2 - 2\dot{\theta}_x\dot{\theta}_z \sin\theta_y) \,]\, ds
\end{aligned} \qquad (A\text{-}1.8)$$

Assuming θ_x, θ_y to be small and noting that $\dot{\theta}_z = \Omega_o$ (the spin speed of shaft), the above expression simplifies to

$$\begin{aligned}
T_e = \frac{1}{2} \int_0^l [\, & m(\dot{x}^2+\dot{y}^2) + I_D(\dot{\theta}_x^2 + \dot{\theta}_y^2) \\
& + I_p(\Omega_o^2 - 2\Omega_o \dot{\theta}_x \theta_y) \,]\, ds
\end{aligned} \qquad (A\text{-}1.9)$$

APPENDIX- II

DERIVATION OF DIFFERENTIAL EQUATIONS BY NEWTONS METHOD

Free body diagram of a differential element of shaft is shown in the Fig.(2.1). Newton's law gives

$$\Sigma F_x = m\bar{a}_x \; ; (Q_x + dQ_x) - Q_x = mds\ \ddot{x}$$

$$\Sigma M_y = \bar{I}\alpha_y ; (M_y + dM_y) - M_y + (Q_x + dQ_x)\frac{ds}{2} + Q_x \frac{ds}{2}$$

$$= \frac{d}{dt}\left(I_D\ ds\ \dot{\theta}_y + I_p\ ds\ \varrho_o\ \theta_x\right) \qquad (A\text{-}2.1)$$

$$\Sigma F_y = m\bar{a}_y \; ; (Q_y + dQ_y) - Q_y = mds\ \ddot{y} \qquad (A\text{-}2.2)$$

$$\Sigma M_x = \bar{I}\alpha_x \; ; \; (M_x + dM_x) - M_x - (Q_y + dQ_y)\frac{ds}{2} - \frac{Q_y}{2} ds$$

$$= \frac{d}{dt}\left[\left(-I_D\ ds\ \dot{\theta}_x + I_p\ ds\ \varrho_o\ \theta_y\right)\right]$$

In these equations M represents bending moment and Q represents shear forces. Suffixes have the usual engineering sense in the right hand coordinate system, other terms have been explained in Chapter 2. Angular momentums are shown in Fig.(A-2.)

Neglecting higher order terms and rearranging, Eqns. (A-2.1) and (A-2.2) become

$$Q_x' = m\ddot{x}$$

$$M_y' + Q_x = I_D \ddot{\theta}_y + I_p \rho_o \dot{\theta}_x \qquad (A\text{-}2.3)$$

$$Q_y' = m\ddot{y}$$

$$M_x' - Q_y = - I_D \ddot{\theta}_x + I_p \rho_o \dot{\theta}_y \qquad (A\text{-}2.4)$$

From mechanics of solids, it is known

$$Q_x = K'GA \left(\frac{\partial y}{\partial s} - \theta_y\right)$$

$$Q_y = K'GA \left(\frac{\partial y}{\partial s} - \theta_x\right) \qquad (A\text{-}2.5)$$

$$M_x = - EI \theta_x' \quad ; \quad M_y = + EI \theta_y' \qquad (A\text{-}2.6)$$

Using these relations, Eqns. (A-2.3) and (A-2.4) become

$$\left[K'GA \left(\frac{\partial x}{\partial s} - \theta_y\right)\right]' - m\ddot{x} = 0$$

$$(EI \theta_y')' + K'GA\left(\frac{\partial x}{\partial s} - \theta_y\right) - I_D\ddot{\theta}_y - I_p \rho_o \dot{\theta}_x = 0 \qquad (A\text{-}2.7)$$

$$\left[K'GA \left(\frac{\partial y}{\partial s} - \theta_x\right)\right] - m\ddot{y} = 0$$

$$(EI \theta_x')' + K'GA\left(\frac{\partial y}{\partial s} - \theta_x\right) - I_D\ddot{\theta}_x + I_p \rho_o \dot{\theta}_y = 0 \qquad (A\text{-}2.8)$$

Equations (A-2.7) to (A-2.8) are exactly the equations (2.9) and (2.10) obtained by Hamilton's principle.

APPENDIX - III

STATIC CONDENSATION

When the mass of a system is assumed to be concentrated at one or few chosen points, the mass matrix will be diagonal. Further, it contains zero diagorial elements for those degrees of freedom, for which there is no associated mass. Whereas the element stiffness matrix formulated by FEM approach is fully populated and relates all the forces to corresponding degrees of freedom. But for those degrees of freedom, for which, the mass matrix contains zero element, the associated inertia forces are zero. Hence, it is necessary to exclude these degrees of freedom from stiffness matrix, for dynamic analysis. The process is called as static condensation (Cough and Penzein [21]) and the procedure is as follows.

Consider a typical matrix equation,

$$\begin{bmatrix} [K_{xx}] & [K_{xy}] \\ [K_{yx}] & [K_{yy}] \end{bmatrix} \begin{Bmatrix} \{x\} \\ \{y\} \end{Bmatrix} = \begin{Bmatrix} \{F_x\} \\ \{0\} \end{Bmatrix} \qquad (A-3.1)$$

where $\{y\}$ represents the column of degrees of freedom to be condensed because the corresponding inertia forces are zero. $\{F_x\}$ represents the inertia forces associated with the degrees of freedom $\{x\}$.

From Eqn. (A-3.1)

$$[K_{xx}]\{x\} + [K_{xy}]\{y\} = \{F_x\} \qquad \text{(A- 3.2)}$$

$$[K_{yx}]\{x\} + [K_{yy}]\{y\} = \{0\} \qquad \text{(A-3.3)}$$

From Eqn. (A-3.3)

$$\{y\} = - [K_{yy}]^{-1} [K_{yx}]\{x\} \qquad \text{(A- 3.4)}$$

Substituting this $\{y\}$ in Eqn. (A-3.2)

$$\left([K_{xx}] - [K_{xy}] [K_{yy}]^{-1} [K_{yx}] \right) \{x\} = \{F_x\} \qquad \text{(A- 3.5)}$$

Thus the degrees of freedom $\{y\}$ are condensed and expressed in terms of $\{x\}$ and the condensed stiffness matrix $[K_c]$ is obtained as

$$[K_c] = \left([K_{xx}] - [K_{xy}][K_{yy}]^{-1} [K_{yx}] \right) \qquad \text{(A-3.6)}$$

REFERENCES

1. Rankine, W.J.M., "Centrifugal Whirling of Shafts", Engineer, Vol. 27, 1869.

2. Robert, G.L. and Vincent, J.F., "Dynamics of Rotating Shafts", The Shock and Vibration Information Center, U.S. Deptt. of Defence, 1969.

3. Tondle, A., "Some problems of Rotor Dynamics", Chapman and Hall, London, 1965.

4. Dimentberg, F.M., "Flexural Vibrations of Rotating Shafts", Butterworths, London, 1961.

5. Rao, J.S., "Rotor Dynamics", Wiley Eastern, New Delhi, 1983.

6. Niordson, F.I., "Dynamics of Rotors", International Symposium, Lingby/Denmark, 1974.

7. Ruhl, R.L. and Booker, J.F., "A Finite Element Model for Distributed Parameter Turborotor Systems", J. of Engg. for Industry, Trans. of ASME, Feb. 1972, P. 126.

8. Nelson, H.D. and McVaugh, J.M., "The Dynamics of Rotor-Bearing Systems Using Finite Elements," J. of Engg. for Industry, Trans. of ASME, May 1976, pp. 593-600.

9. Zorzi, E.S. and Nelson, H.D., "Finite Element Simulation of Rotor- Bearing Systems with Internal Damping", J. of Engg. for Power, Trans. of ASME, Jan. 1977, Vol. 71, pp. 71-76.

10. Kimball, A.L., Newkirk, B.L., "Internal Friction Theory of Shaft Whipping", Gen. Elec. Rev., 1924, vol. 27.

11. Greenhill, L.M., Bickford, W.B. and Nelson, H.D., "A Conical Beam Element for Rotor Dynamics Analysis", J. of Vibration, Acoustics, Stress and Reliability in Design, 1985, vol. 107, pp. 421-429.

12. Lund, J.W., "Stability and Damped Critical Speeds of a Flexible Rotor in Fluid-Film Bearings", Trans. of ASME, J. of Engg. for Industry, 1974, vol. 96, No.2, pp. 507-517.

13. Bansal, P.N. and Kirk, R.G., "Stability and Damped Critical speeds of Rotor-Bearing Systems", J. of Engg. for Industry, Nov. 1975, pp. 1325-1332.

14. Prabhu, B.S. and Ramakrishnan, K.S., "Critical Speeds, Unbalance Response and Onset of Instability of Multispan Multi Rotor systems", National Conference on Industrial Tribology, Hyderabad, Jul. 84.

15. Gupta, D.K.,"Transfer Finite Element Method for Static and Dynamic Problems", M.Tech. Thesis, Department of Mechanical Engg., I.I.T. Kanpur, 1983.

16. Goel, K.S., "Critical Speeds of Rotors by Transfer Finite Element Method", M.Tech. Thesis, Department of Mechanical Engg., I.I.T. Kanpur, Aug. 1986.

17. Meriam, J.L., "Engineering Mechanics, Vol. 1, Statics", John Wiley and Sons, 1980.

18. Crandall, S.H., Dahl, N.C. and Lardner, T.J., "An Introduction to the Mechanics of Solids", Mc. Graw Hill, 1978.

19. Lazan, B.J., "Damping of Materials and Members in Structural Mechanics", Pergamon Press, 1968.

20. Meirovitch, L., "Analytical Methods in Vibrations", Mac Millan Book Co., 1967.

21. Clough, R.W., Penzein, J., "Dynamics of Structures", International Students Edition, McGraw-Hill, 1982.

22. Francis, S.T., Evan, E.M. and Hinkle, T., "Mechanical Vibrations", Prentice/Hall, New Delhi, 1974.
